sequence. We classified identified proteins and genes according to their molecular functions and the cellular components (Fig. 4). It was noticed that many genes encoding ribosomal and plasma membrane proteins were identified in SAGE analysis (Fig. 4d), whereas those proteins were rarely identified in 2-DE analysis (Fig. 4b). Since proteins with extremely high pI or low pI as well as hydrophobic proteins are difficult to be detected by 2-DE in general, obtained expression data were biased in favor of cytoplasmic and soluble proteins.

To evaluate the protein expression, we used the ratio of average spot volume of 2D-DIGE between non HCC and HCC, and the 164 proteins expression were compared to corresponding mRNA expression using the SAGE tag count ratio between non HCC and HCC. The SAGE tag counts were tested by Monte Carlo analysis to determine the statistical significance of expression difference, and a total 40 of 164 proteins showed different mRNA expression significantly ($p \leq 0.05$) between non HCC and HCC. The expression changes of 24 proteins out of 40 between non HCC and HCC seem to be correlated with mRNA expression changes shown as SAGE tag frequency ratio (Fig. 7a, correlation coefficient $r = 0.86$). For example, both mRNA and protein expression of several enzymes abundant in liver, such as alcohol dehydrogenase, acetyl-CoA acyltransferase, and carboxylesterase were reduced (Table 1). Thus, these results suggest that the reduction of these proteins in HCC is regulated transcriptionally. This observation suggests that about 60% of the protein expression difference between non HCC and HCC could be explained by transcriptional regulation. Similar phenomenon of mRNA and protein expression abundance between the different cells was observed in mouse tissue samples [14].

On the other hand, about 30% of the proteins showed opposite expression pattern to the mRNA, and the cellular localization of these opposite group proteins were distinctly different to the similar group proteins. Many opposite group proteins were localized in endoplasmic reticulum, while the similar group proteins were localized in mitochondria (Fig. 8b, d). For example, protein disulfide isomerase A4 and heat shock 70 kDa protein 5 were opposite group proteins (Table 1), and were known as the member of multi-protein complex in mammalian endoplasmic reticulum [20]. Our result suggests that the expression of these proteins was not controlled at transcriptional level in HCC.

Nine multi-spotted proteins showed spot-to-spot variable expression patterns, and some of them were found to be differently modified post-translationally. Indeed, two out of three PGM1 spots were positive for ProQ staining, indicating that these two spots were phosphorylated (Fig. 6). One phosphorylated spot volume was reduced in HCC, whereas non phosphorylated spot volume was increased. The integrated three spot volume of PGM1 did not change between non HCC and HCC, and mRNA expression of PGM1 did not show the significant change between non HCC and HCC. Thus, protein and mRNA expression level of PGM1 per se did not differ between non HCC and HCC, though its phosphorylation level was clearly altered. Recently, PGM1 which is a critical regulator of cellular glucose utilization was shown to be regulated through phosphorylation by p21-activated kinase (Pak1) in a leukemia cell line [5].

The post-translational modification, such as phosphorylation, plays critical roles in cellular signaling, and its detection is expected to provide us to understand molecular basis for cellular functions. Since it is difficult to obtain the information about post-translational modification by mRNA analysis, the combined analysis with both proteome and transcriptome approaches will be important. The protein analysis based on 2-DE technology, which can detect and compare post-translationally modified proteins easily as shown here, is useful for this purpose.

In this study we compared the proteome and the transcriptome profiles from matched HCC and non HCC tissue samples from a single patient. Most of protein expression changes between non HCC and HCC seem to be explained by transcriptional regulation. Further research with a more protein and mRNA expression data of non HCC and HCC samples may yield a general view of the molecular event of HCC.

Acknowledgments We are grateful to Dr. K. Miyazaki and Dr. R. Teramoto for fruitful comments on this work, and N. Tetsura for technical assistance.

References

1. Alban A, David SO, Bjorkesten L, Andersson C, Sloge E, Lewis S, Currie I (2003) Proteomics 1:36–44
2. Berven FS, Karisen OA, Murrell JC, Jensen HB (2003) Electrophoresis 24:757–761
3. Dash S, Saxena R, Myung J, Rege T, Tsuji H, Gaglio P, Garry RF, Thung SN, Gerber MA (2000) J Virol Methods 90:15–23
4. Griffin TJ, Gygi SP, Ideker T, Rist B, Eng J, Hood L, Aebersold R (2002) Mol Cell Proteomics 4:323–333
5. Gururaj A, Barnes CJ, Vadlamudi RK, Kumar R (2004) Oncogene 23:8118–8127
6. Gygi SP, Rochon Y, Franza BR, Aebersold R (1999) Mol Cell Biol 3:1720–1730
7. Iizuka N, Oka M, Yamada-Okabe H, Mori N, Tamesa T, Okada T, Takemoto N, Hashimoto K, Tangoku A, Hamada K, Nakayama H, Miyamoto T, Uchimura S, Hamamoto Y (2003) Oncogene 22:3007–3014
8. Kawai HF, Kaneko S, Honda M, Shirota Y, Kobayashi K (2001) Hepatology 3:676–691
9. Lee IN, Chen CH, Sheu JC, Lee HS, Huang GT, Yu CY, Lu FJ, Chow LP (2005) J Proteome Res 4:2062–2069
10. Liang CR, Leow CK, Neo JC, Tan GS, Lo SL, Lim JW, Seow TK, Lai PB, Chung MC (2005) Proteomics 8:2258–2271

11. Lopez LJ, Marrero JA (2004) Curr Opin Gastroenterol 3:248–253
12. Martin K, Steinberg TH, Cooley LA, Gee KR, Beechem JM, Patton WF (2003) Proteomics 3:1244–1255
13. Midorikawa Y, Makuuchi M, Tang W, Aburatani H (2007) World J Gastroenterol 13:1487–1492
14. Mijalski T, Harder A, Halder T, Kersten M, Horsch M, Strom TM, Liebscher HV, Lottspeich F, de Angelis MH, Beckers J (2005) Proc Natl Acad Sci USA 102:8621–8626
15. Saha S, Sparks AB, Rago C, Akmaev V, Wang CJ, Vogelstein B, Kinzler KW, Velculescu VE (2002) Nat Biotechnol 5:508–512
16. Seow TK, Liang RCMY, Leow CK, Chung MCM (2001) Proteomics 1:1249–1263
17. Shackel NA, Seth D, Haber PS, Gorrell MD, McCaughan GW (2006) Comp Hepatol 5:6
18. Stahl S, Ittrich C, Marx-Stoelting P, Köhle C, Altug-Teber O, Riess O, Bonin M, Jobst J, Kaiser S, Buchmann A, Schwarz M (2005) Hepatology 2:353–361
19. Steinberg TH, Agnew BJ, Gee KR, Leung WY, Goodman T, Schulenberg B, Hendrickson J, Beechem JM, Haugland RP, Patton WF (2003) Proteomics 3:1128–1144
20. Stockton JD, Merkert MC, Kellaris KV (2003) Biochemistry 42:12821–12834
21. Unlu M, Morgan ME, Minden JS (1997) Electrophoresis 11:2071–2077
22. Yamashita T, Kaneko S, Hashimoto S, Sato T, Nagai S, Toyoda N, Suzuki T, Kobayashi K, Matsushima K (2001) Biochem Biophys Res Commun 282:647–654
23. Zanella I, Rossini A, Domenighini D, Albertini A, Cariani E (2002) J Med Virol 68:494–499

Optimal amount of monocyte chemoattractant protein-1 enhances antitumor effects of suicide gene therapy against hepatocellular carcinoma by M1 macrophage activation

Tomoya Tsuchiyama,[1] Yasunari Nakamoto,[1] Yoshio Sakai,[1] Naofumi Mukaida[2] and Shuichi Kaneko[1,3]

[1]Disease Control and Homeostasis, Graduate School of Medical Science, [2]Division of Molecular Bioregulation, Cancer Research Institute, Kanazawa University, 13-1 Takara-machi, Kanazawa 920-8641, Japan

(Received April 10, 2008/Revised June 18, 2008/Accepted June 27, 2008)

Suicide gene therapy combined with chemokines provides significant antitumor efficacy. Coexpression of suicide gene and monocyte chemoattractant protein-1 (MCP-1) increases antitumor effects in murine models of hepatocellular carcinoma (HCC) and colon cancer. However, it is unclear whether the doses administered achieved the maximum antitumor effects. We evaluated antitumor effects of various amounts of recombinant adenovirus vector (rAd) expressing MCP-1 in the presence of a suicide gene in a murine model of HCC. HCC cells were transplanted subcutaneously into BALB/c nude mice, and transduced with a fixed amount of Ad-tk harboring the suicide gene, *HSV-tk*, and various doses of Ad-MCP1 harboring MCP-1 (ratios of 1:1, 0.1:1, and 0.01:1 relative to Ad-tk). Growth of primary tumors was suppressed when treated with Ad-tk plus Ad-MCP1 (1:1 and 1:0.1) as compared with Ad-tk alone. The antitumor effects against tumor rechallenge tended to be high in the Ad-tk plus Ad-MCP1 group (1:0.1). The effects were dependent on production of Th1 type-cytokines. Delivery of an optimal amount of rAd expressing MCP-1 enhanced the antitumor effects of suicide gene therapy against HCC by M1 macrophage activation, suggesting that this is a plausible form of cancer gene therapy to prevent HCC progression and recurrence. (*Cancer Sci* 2008)

Cancer gene therapy using combinations of various genes, such as suicide and cytokine genes, to enhance tumor regression therapy is widely used.[1,2] Previously, we reported that the coexpression of herpes simplex virus thymidine kinase (HSV-tk) and monocyte chemoattractant protein-1 (MCP-1) showed enhanced antitumor effects in models of hepatocellular carcinoma (HCC)[3] and colon cancer,[4] and these antitumor effects were dependent on the activation of macrophages.[3] MCP-1 is a chemokine that regulates the recruitment of monocytes/macrophages to inflammatory sites and tumor tissues as well as their activation, including lysosomal enzyme release and tumoricidal activity,[5] and is functional in both mice and humans.[6] However, MCP-1 was reported to be destructive in some tumor models,[6,7] but protective in others.[8] Monocytes/macrophages recruited by MCP-1 have dual functions in that they can prevent the establishment and spread of tumor cells,[6] and simultaneously support tumor growth and dissemination.[8] This ambivalent relationship reflects the elevated functional plasticity of macrophages, which are able to express different functional programs in response to different microenvironment signals, as exemplified in the M1 (classical)–M2 (alternative or non-classical) paradigm of macrophage polarization.[9]

On the other hand, although double infection methods are used to enhance antitumor effects in cancer gene therapy, significant antitumor effects have been reported in some studies,[4,10] but not in others.[11,12] Moreover, it is not clear how the antitumor effects are affected by differences in the doses administered. In the present study, various amounts of recombinant adenovirus vector (rAd) expressing the *MCP-1* gene were delivered into cells along with the same amount of HSV-tk to determine the optimal dosage of MCP-1 for induction of stronger antitumor effects in double infection methods. Furthermore, we also examined the involvement of macrophage immune responses in these effects. Here, we demonstrated that treatment with the 1:0.1 ratio of Ad-HSV-tk (Ad-tk) plus Ad-MCP1 tended to exert antitumor immunity, suggesting that there may be an optimal amount of Ad-MCP1 in suicide gene therapy. In addition, it is possible that the antitumor responses seen in the HSV-tk plus MCP-1 system were associated with increased Th1 (T helper 1)–type cytokine production by activated M1 macrophage. These findings will be of value in cancer gene therapy.

Materials and Methods

Recombinant adenoviruses. rAds harboring the human MCP-1 (Ad-MCP1), HSV-tk (Ad-tk), and lacZ (Ad-lacZ), and driven by the CAG promoter were prepared, purified, and titrated according to the protocols supplied by the manufacturer (Takara Bio, Shiga, Japan), as described.[13] The rAds were purified on cesium gradients and their titers were determined by the 50% tissue culture infectious dose ($TCID_{50}$).

Cell lines and culture. The human HCC cell line Huh7 and the mouse HCC cell line BNL 1ME A.7R.1 (BNL) were cultured in Dulbecco's minimal essential medium (Gibco, Long Island, NY, USA) supplemented with 10% heat-inactivated fetal bovine serum (Gibco).

Enzyme-linked immunosorbent assay (ELISA) for MCP-1. Aliquots of 1×10^5 Huh7 cells were seeded in 1.0 mL of culture media in 24-well tissue culture plates. Twenty-four h later, the cells were infected with each rAd at a multiplicity of infection (MOI) of 10, and the medium was collected 48 h later. On the other hand, in some experiments, ganciclovir (GCV; Tanabe Pharmaceutical Drug, Tokyo, Japan) (10 μg/mL) was added 72 h later, and the medium was collected and replaced with the same volume of fresh medium every 24 h. The concentration of MCP-1 in the medium collected from each well was determined by ELISA as described.[14]

***In vivo* studies in nude mice.** The following investigations were performed in accordance with the guidelines of our Institutional Animal Care and Use Committee. Six-week-old male athymic

[3]To whom correspondence should be addressed. E-mail: skaneko@m-kanazawa.jp

doi: 10.1111/j.1349-7006.2008.00951.x

nude mice (BALB/cA Jcl-nu; CLEA Japan, Tokyo, Japan) were injected subcutaneously with 1×10^7 HuH7 cells at the both sides of the flank on day 0. On days 3 and 4, 1×10^7 $TCID_{50}$ (100 μL) of Ad-tk, Ad-lacZ, or Ad-tk (1×10^7 $TCID_{50}$, fixed dose) plus Ad-MCP1 (1, 0.1, 0.01, or 0.001×10^7 $TCID_{50}$, changed dose) were injected into the tumor. Then, 75 mg/kg of GCV was administered into the peritoneal cavity daily for the next 5 consecutive days (day 5–9), and tumor size was measured every 3 days. Tumor volumes were calculated using the formula:

$$\frac{(\text{longest diameter}) \times (\text{shortest diameter})^2}{2}$$

Gene expression analysis (real-time reverse transcription–polymerase chain reaction [RT-PCR]). Total RNA was extracted from tumor tissues or spleens resected after treatment of the tumor with each rAd, using a Total Cellular RNA Isolation Kit (Ambion, St. Austin, TX, USA), in accordance with the manufacturer's protocol. The RNA was reverse transcribed with a TaqMan reverse transcription reagent kit (PE Applied Biosystems, Foster City, CA, USA) using random hexamer primers. Gene expression was analyzed by real-time RT-PCR using TaqMan Universal Master Mix on an ABI PRISM 7900 Sequence Detection System (PE Applied Biosystems). The PCR primer pairs for mouse interleukin (IL)–10, IL-12, IL-18, IFN-γ, VEGF, and 18S rRNA were obtained from the TaqMan assay reagent library. Data for whole samples were normalized to 18S rRNA and then expressed as the fold change in mRNA expression as compared with control samples treated with phosphate-buffered saline (PBS).

Immunohistochemical analysis. Tumor tissues were resected on day 10. The tissue samples were embedded in OCT compound (Sakura Finetek, Torrance, CA, USA) and snap-frozen in liquid nitrogen. Cryostat sections of frozen tissues were fixed in cold acetone for 10 min, followed by three rinses in PBS. To avoid non-specific staining, avidin and biotin in the tissues were blocked using a blocking kit (Vector Laboratories, Burlingame, CA, USA). The slides were subsequently incubated with antibodies (Abs) against Mac-1 (M1/70; Pharmingen, San Diego, CA, USA) for 30 min at room temperature. Negative controls included staining with non-specific Ab of the corresponding isotype and subsequent staining with secondary Ab. The reactions were visualized using a VECTASTAIN ABC Standard Kit (Vector Laboratories), followed by counterstaining with hematoxylin.

Preparation of peritoneal exudate macrophages and assays for cytokine production *in vitro*. Thioglycolate-elicited murine peritoneal exudate cells were collected as described.[15] Briefly, nude or immunocompetent mice were injected intraperitoneally with 2 mL each of 3% fluid thioglycolate medium (Wako Pure Chemical) and sacrificed 4 days later, followed by peritoneal lavage with 10 mL of cold PBS. About 90% of the collected peritoneal cells were positive for both Mac-1 (CD11b) and $I\text{-}A^d$ MHC class II as determined by staining with PE-conjugated anti-Mac-1 Ab and fluorescein-isothiocyanate (FITC)–conjugated $I\text{-}A^d$ MHC class II (AMS-32.1; Pharmingen). Huh7 cells were infected with rAds, at a MOI of 5 for 24 h. Aliquots of 10^5 macrophages were cocultured with 10^5 rAd-treated Huh7 cells in 1.0 mL of culture media in 24-well tissue culture plates, and treated with GCV for 2 days at 37°C. The concentrations of IL-10, IL-12, IL-18, and IFN-γ in the media were quantified using immunoassay kits (IL-10, IL-12, IFN-γ: Biosource International, Camarillo, CA, USA; IL-18: Medical & Biological Laboratories, Nagoya, Japan).

Rechallenge testing in nude mice. Nude mice were injected subcutaneously with 5×10^6 HuH7 cells on day 0. On days 3 and 4, the subcutaneous tumors were injected with 5×10^7 $TCID_{50}$ (100 μL) of Ad-tk, Ad-lacZ, or Ad-tk (fixed dose) plus Ad-MCP1 (changed dose), and the mice were treated with 75 mg/kg GCV, injected into the peritoneal cavity, every day for the next 5 days (days 5–9). Following complete eradication of the primary tumors, the mice were subcutaneously rechallenged on day 14 with 3×10^6 HuH7 cells at two sites, which were more than 3 cm apart from the primary challenge site. Two of 10 (20%) mice treated with Ad-tk and four of 30 (13.3%) treated with Ad-tk plus Ad-MCP1 did not show complete eradication of the primary tumor by the final measurement and were therefore excluded from the rechallenge experiment. Tumor sizes were measured every 4 days after the second tumor injection, and tumor volumes were calculated using the formula:

$$\frac{(\text{longest diameter}) \times (\text{shortest diameter})^2}{2}$$

Animal studies in immunocompetent mice (*ex vivo*, *in vivo*, and rechallenge). Six-week-old immunocompetent male BALB/c-jcl mice (CLEA Japan) were injected subcutaneously with 1×10^5 BNL cells infected with each rAd at an *in vitro* MOI of 5 at the both sides of the flank on day 0, and GCV was administered intraperitoneally for the next 5 days (days 1–5). Tumor size was measured every 7 days, and tumor volume was calculated using the formula:

$$\frac{(\text{longest diameter}) \times (\text{shortest diameter})^2}{2}$$

As with the experiments on nude mice, BALB/c-jcl mice were injected subcutaneously with 1×10^5 BNL cells at the both sides of the flank on day 0. On days 3 and 4, 5×10^5 $TCID_{50}$ (100 μL) of rAds were injected into the tumor. Then, GCV was administered for the next 5 days (day 5–9), and tumor size was measured every 3 days.

In another experiment, immunocompetent mice were injected subcutaneously with 1×10^5 BNL cells infected with each rAd at an *in vitro* MOI of 100 on day 0, and GCV was administered intraperitoneally for the next 5 days (days 1–5). The primary tumors were completely eradicated in all groups. These mice were injected subcutaneously with 1×10^4 BNL cells on day 14 at two sites which were separate from the primary challenge sites, and the tumor sizes were measured every 7 days after the second tumor injection.

ELISA for serum IL-10, IL-12, and IL-18. Mouse sera were collected prior to injection of subcutaneous primary tumors and on day 35 after tumor injection. IL-10, IL-12, and IL-18 concentrations were measured using immunoassay kits (IL-12, Biosource International; IL-18, Medical & Biological Laboratories).

Flow cytometry. Single-cell suspensions of splenocytes were resuspended in PBS containing 1% bovine serum albumin and 0.1% sodium azide, and incubated for 30 min on ice with FITC-conjugated rat antimouse-F4/80 (Serotec, Oxford, UK) and PE-conjugated rat antimouse pan natural killer (NK) cells (DX5; Pharmingen), with FITC-conjugated rat antimouse-CD3 (Pharmingen) and PE-conjugated rat antimouse CD11c (Pharmingen) or with FITC-conjugated rat antimouse-CD8 (Pharmingen) and PE-conjugated rat antimouse CD4 (Pharmingen). The cells were washed, resuspended in PBS, and analyzed using a FACScan with CellQuest software.

Statistical analysis. All results are expressed as means ± SE. The statistical significance of differences between groups was evaluated by the Mann–Whitney *U*-test.

Results

MCP-1 production by double infection with recombinant adenoviruses *in vitro*. MCP-1 expression level by Ad-MCP1 alone was high compared with double infection of Ad-lacZ plus Ad-MCP1 (Fig. 1a). The amounts of MCP-1 produced by Ad-tk plus Ad-MCP1 decreased rapidly after GCV administration due to Huh7 cell

doi: 10.1111/j.1349-7006.2008.00951.x

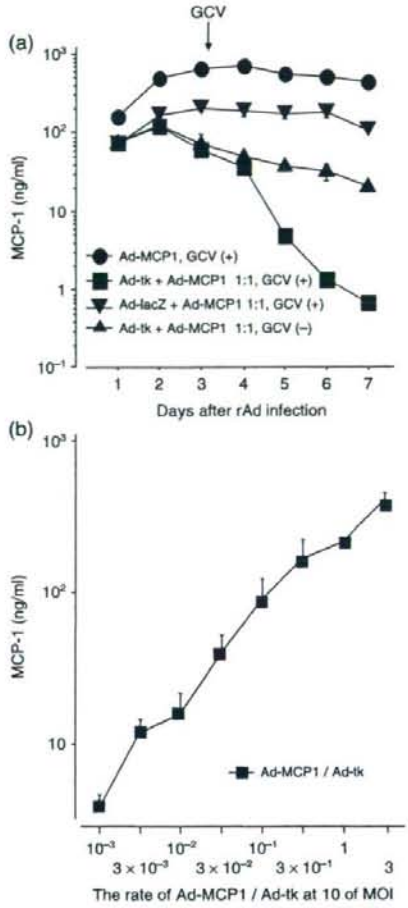

Fig. 1. Monocyte chemoattractant protein-1 (MCP-1) production of recombinant adenoviruses in the presence of herpes simplex virus thymidine kinase (HSV-tk). Aliquots of 1×10^5 Huh7 cells were seeded in 1.0 mL of culture media in 24-well tissue culture plates. (a) Twenty-four h later, the cells were treated with Ad-tk plus Ad-MCP1, Ad-lacZ plus Ad-MCP1, or Ad-MCP1 at a multiplicity of infection (MOI) of 10, and treated 72 h later with ganciclovir (GCV) (10 μg/mL). Every 24 h, the medium was collected and replaced with the same volume of fresh medium. (b) Twenty-four h later, the cells were doubly infected with Ad-tk (fixed dose, at an MOI of 10) plus Ad-MCP1 (changed dose), and the medium was collected 48 h later. The concentrations of MCP-1 were evaluated using an immunoassay. Values are shown as the means ± SE of duplicate experiments.

apoptosis induced by the HSV-tk/GCV system (Fig. 1a). Moreover, the amounts of MCP-1 produced by Ad-tk plus Ad-MCP1 without GCV administration were lower than those of Ad-lacZ plus Ad-MCP1, presumably due to the MCP-1 promoter interference by HSV-tk.

Next, production of MCP-1 in Huh7 cells double-infected with Ad-tk (fixed dose) plus Ad-MCP1 (changed dose) was measured. The amounts of MCP-1 were correlated with the infectious dose of Ad-MCP1 in the presence of a fixed amount of HSV-tk (Fig. 1b).

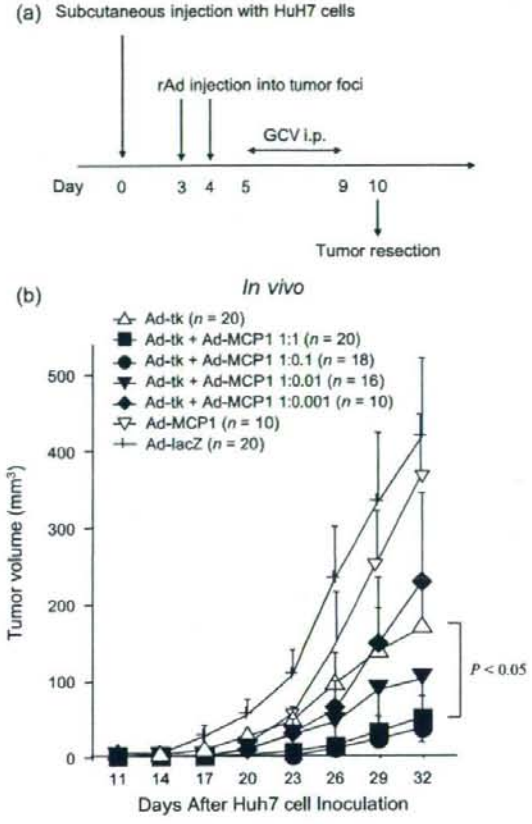

Fig. 2. The antitumor effects of the herpes simplex virus thymidine kinase (HSV-tk)/ganciclovir (GCV) system by codelivery of monocyte chemoattractant protein-1 (MCP-1) in a nude mouse model of hepatocellular carcinoma (HCC). (a) Mice were injected subcutaneously with 1×10^7 Huh7 cells at the both sides of the flank on day 0. On days 3 and 4, 1×10^7 $TCID_{50}$ of Ad-tk, Ad-tk (1×10^7 $TCID_{50}$, fixed dose) plus Ad-MCP1 (1, 0.1, 0.01, or 0.001×10^7 $TCID_{50}$, changed dose), or Ad-lacZ was injected into the tumor, and the mice were injected intraperitoneally (i.p.) with 75 mg/kg of GCV every day for the next 5 days (day 5–9). (b) Tumor size was measured every 3 days. The results are shown as the means of two independent experiments.

Antitumor effects of the HSV-tk/GCV system by codelivery of the *MCP-1* gene in an athymic nude mouse model of HCC. The *in vivo* antitumor effects of double infection with rAds were analyzed using athymic nude mice (Fig. 2a). The growth of subcutaneous tumors was markedly suppressed in animals treated with Ad-tk plus Ad-MCP1 (1:1) (tumor volume 32 days after injection, 44.4 ± 22.5 mm^3) or Ad-tk plus Ad-MCP1 (1:0.1) (37.4 ± 18.6 mm^3), as compared to those treated with Ad-tk alone (170.2 ± 49.8 mm^3, $P < 0.05$) (Fig. 2b). These observations indicated that optimal amounts of MCP-1 are needed to eradicate tumor cells in the presence of HSV-tk.

Recruitment and activation of macrophages into tumor tissues. Macrophages play important roles in both Th1- and Th2-mediated immune responses. Classical macrophage (M1 macrophages) are also a major source of IL-12 and IL-18, whereas alternative macrophages (M2 macrophages) are a source of IL-10.[9] IL-12

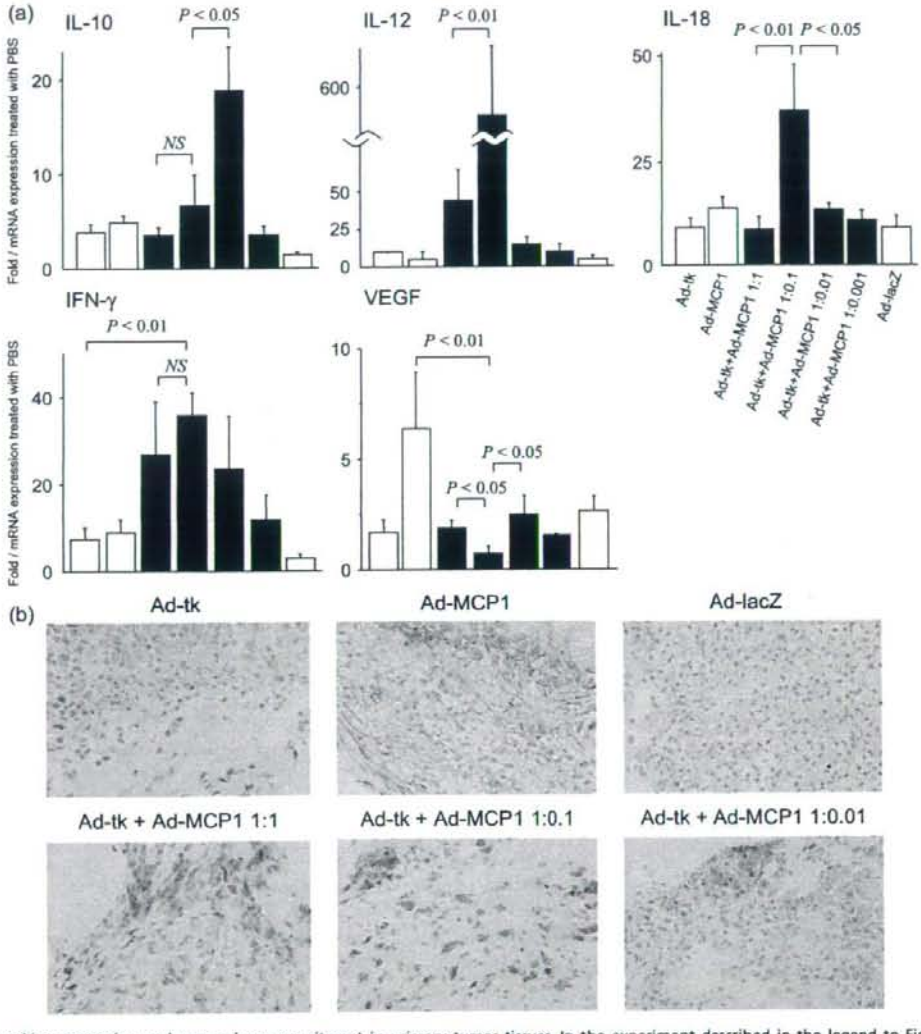

Fig. 3. Cytokine expression and macrophage recruitment in primary tumor tissues. In the experiment described in the legend to Fig. 2, tumor tissues were resected 10 days after tumor injection. (a) Total RNA was extracted to determine cytokine mRNA levels by a real-time reverse transcription–polymerase chain reaction as described in 'Materials and Methods'. Cytokine mRNA expression was normalized to 18S rRNA and then expressed as the fold change in mRNA expression as compared with control samples treated with phosphate-buffered saline. Splenocytes treated with 0.1 μg/mL LPS were used as a positive control (data not shown). The results are shown as the means of two independent experiments. (b) Tumor tissues were processed for immunohistochemical analysis using anti-Mac1 antibody as described in 'Materials and Methods'. Representative results from individual animals in each group are shown here.

enhances the activities of NK cells and cytotoxic T lymphocytes (CTL), and plays a key role in the induction of Th1-type immune responses.[16] In addition, IL-18 is a proinflammatory cytokine produced by activated macrophages, which has been shown to induce Th1 cell development and NK cell activation in combination with IL-12.[17] In contrast, the effects of IL-10 on immune responses are mostly inhibitory.[18] Therefore, to evaluate whether M1 macrophages recruited into tumor tissues following infection with rAds were activated, IL-10, IL-12, IL-18, IFN-γ, and VEGF expression were determined using real-time RT-PCR. IL-12 and IL-18 mRNA levels were significantly increased ($P < 0.01$), and that of IFN-γ mRNA tended to increase in tumors treated with Ad-tk plus Ad-MCP1 (1:0.1) (Fig. 3a). In contrast, IL-10 mRNA was significantly increased in tumors treated with Ad-tk plus Ad-MCP1 (1:0.01) ($P < 0.05$) (Fig. 3a). In addition, the VEGF mRNA level was significantly increased in tumors treated with Ad-MCP1 ($P < 0.01$), and was significantly decreased in tumors treated with Ad-tk plus Ad-MCP1 (1:0.1)

doi: 10.1111/j.1349-7006.2008.00951.x

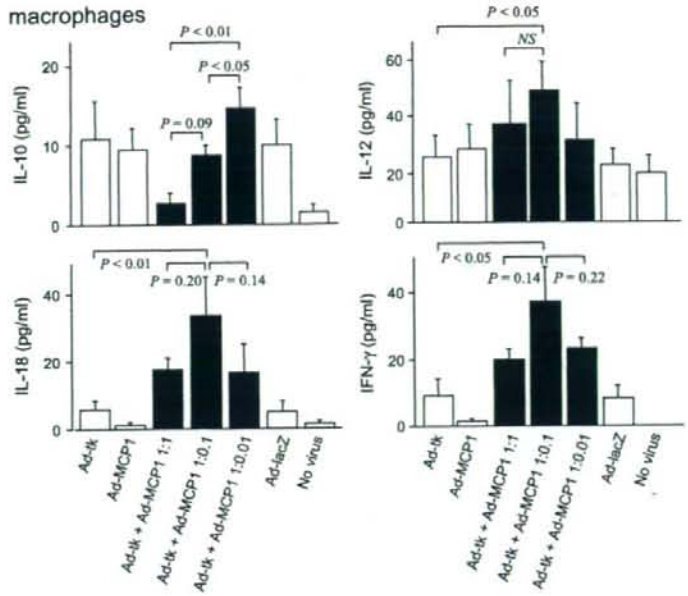

Fig. 4. Cytokine production by peritoneal macrophages cocultured with Huh7 cells infected with rAds *in vitro*. Huh7 cells were infected with each rAd at a multiplicity of infection (MOI) of 5 and treated with ganciclovir (GCV) for 24 h. Aliquots of 10^5 peritoneal exudate macrophages were cocultured with 10^5 rAd-treated Huh7 cells for 2 days, and the concentrations of IL-10, IL-12, IL-18, and IFN-γ in the media were evaluated by immunoassay. Values are shown as the means ± SE of duplicate experiments.

($P < 0.05$) (Fig. 3a). Taken together, these observations indicated that M1 macrophages were highly activated when tumors were treated with the optimal dose of MCP-1 and HSV-tk.

Next, we evaluated whether there were differences in the number of macrophages recruited into tumor tissues. The number of accumulated Mac-1-positive cells in the tumors treated with Ad-tk plus Ad-MCP1 (1:0.1) was comparable to that in those treated with Ad-tk plus Ad-MCP1 (1:1) (Fig. 3b). These observations suggested that the number of recruited macrophages is of little importance to the antitumor effects.

IL-10, IL-12, IL-18, and IFN-γ production by coculture of apoptotic Huh7 cells expressing MCP-1 and peritoneal macrophages *in vitro*. It was reported that adenoviral-mediated overexpression of MCP-1 differentially modulated the development of Th1 and Th2–type responses.[19] To evaluate the differences in the immunomodulatory effects of macrophages among double infection of rAds, we measured IL-10, IL-12, IL-18, and IFN-γ production by peritoneal exudate cells consisting mostly of macrophages, when they were cocultured with Huh7 cells infected with rAds. We found that peritoneal macrophages cocultured with Huh7 cells treated with Ad-tk plus Ad-MCP1 (1:0.1) tended to produce increased levels of IL-12, IL-18, and IFN-γ (Fig. 4). On the other hand, the increase in amount of IL-10 in the double infection groups was inversely proportional to the dosage of MCP-1 vector (Fig. 4). These observations also suggest that the optimal dose of MCP-1 and HSV-tk may induce M1 macrophage activation.

Antitumor immunity in the rechallenge test of the HSV-tk/GCV system by codelivery of the *MCP-1* gene. After primary subcutaneous Huh7 cells were completely eradicated with rAds, nude mice were rechallenged with Huh7 cells to evaluate antitumor immunity induced by MCP-1 plus HSV-tk. We found that the tumor regrowth was significantly suppressed when the primary tumor cells had been eradicated with Ad-tk plus Ad-MCP1 (1:0.1) as compared with Ad-tk (tumor volume 40 days after rechallenge: 123.2 ± 77.2 mm^3 *vs* 544.5 ± 161.6 mm^3, respectively, $P < 0.05$) (Fig. 5). In addition, tumor regrowth tended to be low when eradicated with Ad-tk plus Ad-MCP1 (1:0.1) as compared with Ad-tk plus Ad-MCP1 (1:1) (287.9 ± 137.1 mm^3, $P = 0.18$) or Ad-tk plus Ad-MCP1 (1:0.01) (269.7 ± 91.1 mm^3, $P = 0.24$). Next, to evaluate immunomodulatory effects of splenocytes, we examined IFN-γ expression using real-time RT-PCR. IFN-γ mRNA levels were significantly increased in the spleens of nude mice treated with Ad-tk plus Ad-MCP1 (1:0.1) (Fig. 5b). Consistent with our previous findings,[20] we observed increased numbers of NK cells in the spleen and rechallenged tumor tissues when treated with the 1:0.1 ratio of Ad-tk and Ad-MCP1 (data not shown). These results indicated that the optimal dose of MCP-1 induced beneficial antitumor immunity in the presence of HSV-tk.

Antitumor effects and immunity of the HSV-tk/GCV system plus MCP-1 treatment in an immunocompetent mouse model of HCC. There is no CTL in athymic nude mice. Therefore, to evaluate the Th1 cytokine response in the syngeneic system, the *ex vivo* antitumor effects of double infection with rAds were analyzed using immunocompetent BALB/c-jcl mice. The growth of subcutaneous tumors treated with Ad-tk plus Ad-MCP1 (1:1, 1:0.1) was comparable to that in nude mice ($P < 0.01$), excluding the group in which the dose of MCP-1 was small (1:0.01) (Fig. 6a).

In the next experiment, after the BALB/c mice developed tumor mass following the injection with non-infected BNL cells, we infected the resultant tumors with Ad-tk plus Ad-MCP1 and treated the animals with GCV using the same procedures as the experiments with nude mice. Tumor growth was apparently retarded when treated with Ad-tk plus Ad-MCP1 (1:1) ($P < 0.05$) and (1:0.1) ($P < 0.01$) as compared with Ad-tk alone (Fig. 6b). However, the treatments failed to eradicate tumors completely, probably because the infection efficiency was not sufficient under these conditions.

Thus, we chose the *ex vivo* infection experiment in the immunocompetent mouse model, to evaluate whether rechallenged tumors could be rejected in the mice in which the primary tumors had been completely eradicated. The immunocompetent mice were rechallenged with BNL 1ME A.7R.1 (BNL) cells

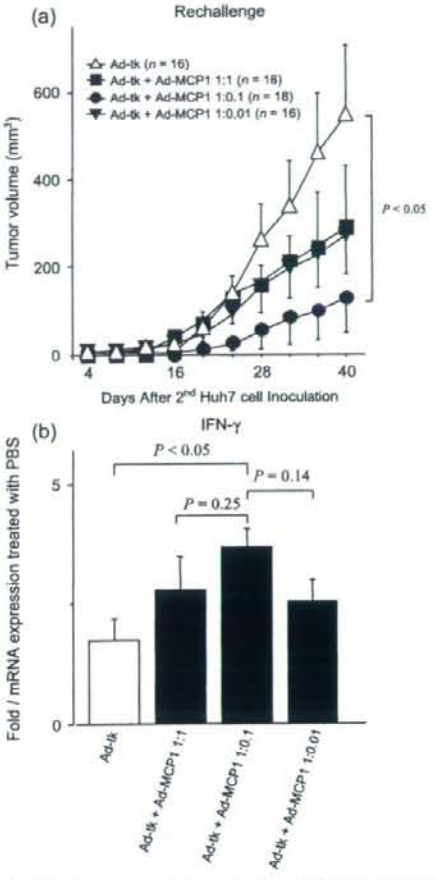

Fig. 5. Nude mice were injected subcutaneously with 5×10^6 Huh7 cells on day 0. On days 3 and 4, 5×10^7 $TCID_{50}$ of Ad-tk (100 μL), Ad-tk (1×10^7 $TCID_{50}$, fixed dose) plus Ad-MCP1 (1, 0.1, 0.01, or 0.001×10^7 $TCID_{50}$, changed dose), or Ad-lacZ was injected into the tumor, and the mice were injected intraperitoneally with 75 mg/kg of ganciclovir (GCV) every day for the next 5 days (day 5–9). Following complete eradication of the primary tumors, the mice were subcutaneously rechallenged on day 14 with 3×10^6 Huh7 cells at the other sites. (a) Tumor size was measured every 4 days. (b) In another series of experiments, the spleen was resected on day 16 after tumor injection, and IFN-γ, mRNA levels were evaluated using real-time reverse transcription–polymerase chain reaction. The results are shown as the means of two independent experiments. PBS, phosphate-buffered saline.

using the same procedures as in the experiments with nude mice. Although the inhibition of tumor regrowth was significantly lower when they had been eradicated with Ad-tk plus Ad-MCP1 (1:0.1) as compared with Ad-tk (tumor volume 42 days after rechallenge: 263.9 ± 87.8 mm³ *vs* 669.5 ± 158.3 mm³, respectively, $P < 0.05$), it also tended to be lower when the primary tumor cells had been eradicated with Ad-tk plus Ad-MCP1 (1:1) (tumor volume 42 days after rechallenge: 372.5 ± 157.8 mm³) (Fig. 6c), similar to the observations in athymic nude mice.

Next, we examined IL-10, IL-12, and IL-18 production on day 35 after tumor injection. Serum concentrations of IL-12 and IL-18 tended to be higher in mice treated with Ad-tk plus Ad-MCP1 (1:0.1) as compared with those treated with Ad-tk, Ad-tk plus Ad-MCP1 (1:1), or Ad-tk plus Ad-MCP1 (1:0.01) (Fig. 6d). In contrast, the increase in amount of serum IL-10 in the double infection groups was inversely proportional to the dosage of MCP-1 (Fig. 6d). These observations were consistent with the data shown in Figs 3 and 4.

Finally, to monitor the activation state of innate and acquired immunity in extrahepatic lymphoid organs, we examined the numbers of immune cells in the spleen on day 35 after tumor injection by FACS analysis. The numbers of F4/80-positive cells tended to be higher in the Ad-tk plus Ad-MCP1 (1:1) and Ad-tk plus Ad-MCP1 (1:0.1) groups, and the numbers of DX5-positive cells tended to be higher in the Ad-tk plus Ad-MCP1 (1:0.1) group (Fig. 6e). Furthermore, the numbers of CD3-, CD4-, and CD8-positive cells were increased in the immunocompetent mice in the order of Ad-tk plus Ad-MCP1 (1:0.1), Ad-tk plus Ad-MCP1 (1:1), and Ad-tk plus Ad-MCP1 (1:0.01) (Fig. 6e). Taken together, these results confirmed that treatment with Ad-tk plus Ad-MCP1 (1:0.1) resulted in the development of beneficial antitumor immunity in both immunodeficient and immunocompetent animals.

Discussion

HCC is one of the most common cancer-related causes of death, and is resistant to anticancer drugs.[21] Although gene therapy has the potential to more effectively induce tumor cell death as compared to conventional treatment, there have been no previous comparisons with regard to the optimal doses of vectors in combined gene therapy. Whereas the amounts of MCP-1 were correlated with the infectious dose of Ad-MCP1 in the presence of a fixed dose of Ad-tk, MCP-1 expression level in the presence of intracellular HSV-tk was inhibited as compared with coinfection with Ad-MCP1 plus Ad-lacZ, suggesting that HSV-tk may influence the efficiency of transcription in the transformed cells. In addition, MCP-1 expression level by Ad-MCP1 alone was high as compared with double infection with Ad-MCP1 plus Ad-lacZ, which was probably due to promoter interference. On the other hand, our previous study demonstrated that the levels of HSV-tk expression in cells cotransfected with Ad-tk plus Ad-MCP-1 were comparable to those of Ad-tk alone or Ad-tk plus Ad-lacZ.[3] The effect of a bicistronic rAd expressing mainly HSV-tk was clearly stronger than that of a bicistronic rAd expressing mainly MCP-1. Therefore, we proposed that the

Fig. 6. Antitumor effects of the herpes simplex virus thymidine kinase (HSV-tk)/ganciclovir (GCV) system by codelivery of monocyte chemoattractant protein-1 (MCP-1) in an immunocompetent mouse model of HCC. (a) Mice were injected subcutaneously with 1×10^5 BNL cells infected with each rAd at an *in vitro* multiplicity of infection (MOI) of 5 at the both sides of the flank on day 0. GCV was administered intraperitoneally for the next 5 days (days 1–5), and tumor size was measured every 7 days. (b) BALB/c-jcl mice were injected subcutaneously with 1×10^5 BNL cells at the both sides of the flank on day 0. On days 3 and 4, 5×10^5 $TCID_{50}$ (100 μL) of rAds were injected into the tumor. Then, GCV was administered for the next 5 days (day 5–9), and tumor size was measured every 3 days. (c) BALB/c-jcl mice were injected subcutaneously with 1×10^5 BNL cells infected with each rAd at an *in vitro* MOI of 100 on day 0, and GCV was administered intraperitoneally for the next 5 days (days 1–5). The primary tumors were completely eradicated in all groups. These mice were injected subcutaneously with 1×10^4 BNL cells at other sites on day 14, and the tumor sizes were measured every 7 days after the second tumor injection. (d) Mouse sera were collected prior to subcutaneous injection of primary tumor cells (untreated), after treatment of the tumor with each rAd, and 2 days after rechallenge with HuH7 cells, and IL-12 and IL-18 concentrations were measured using immunoassay kits. (e) The spleen was removed to obtain single cell suspensions on day 35 after tumor injection. Surface expression of DX5, F4/80, CD3, CD4, CD8, and CD11c in cell populations obtained from the spleen were assessed by FACS. The results are representative of two independent experiments.

doi: 10.1111/j.1349-7006.2008.00951.x

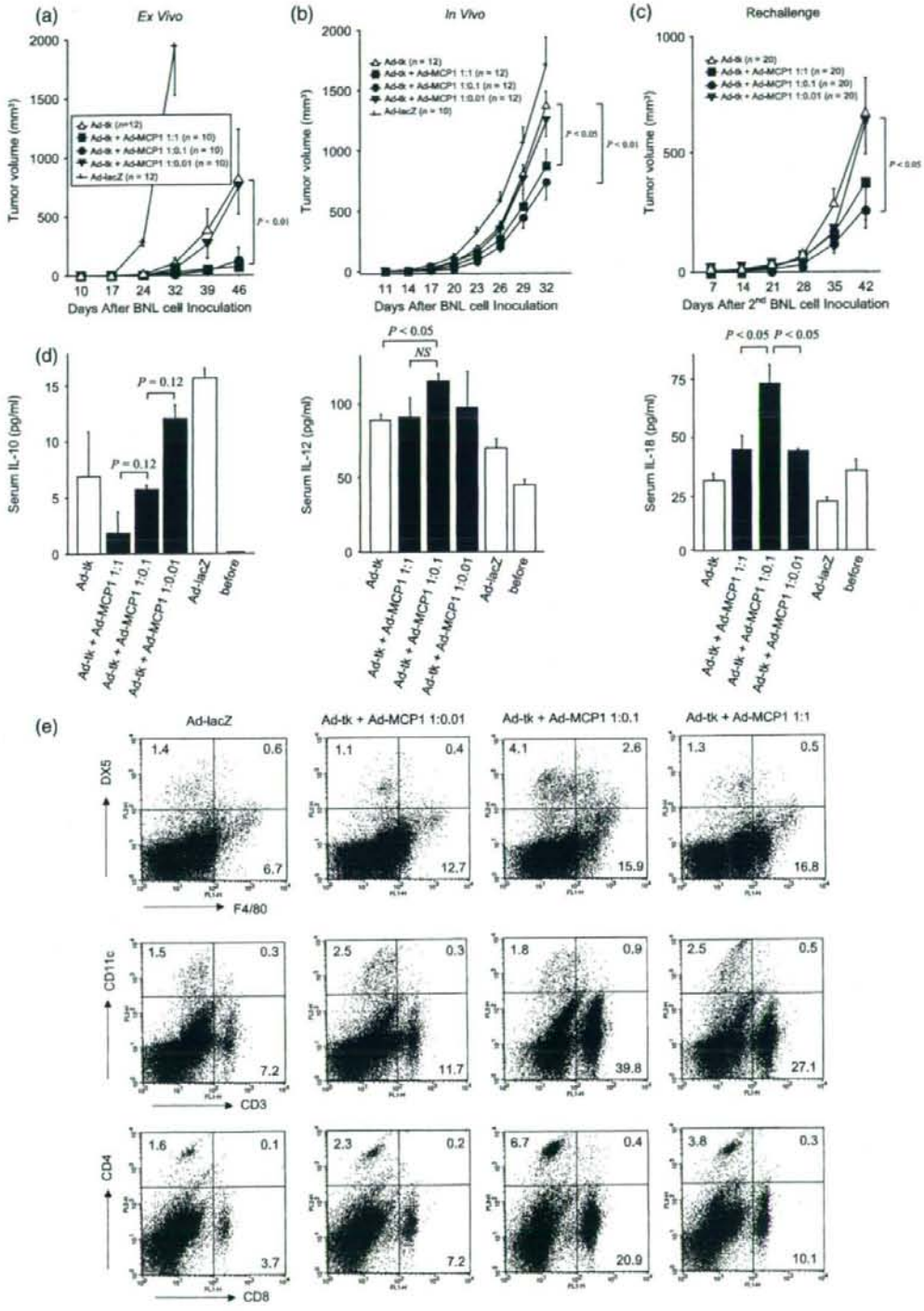

HSV-tk/GCV system should mainly be used and the use of MCP-1 was supported in our experimental models, although their efficiencies may vary depending on the nature of the cell type and reporter genes used.[22]

Th1 cytokine expression levels in tumors treated with Ad-tk plus Ad-MCP1 (1:0.1) were higher than those treated with Ad-tk plus Ad-MCP1 (1:1) or (1:0.01). Moreover, macrophages produced large amounts of Th1 cytokines when cocultured with apoptotic HCC cells induced by Ad-tk plus Ad-MCP1 (1:0.1). In contrast, whereas the amounts of Th2 cytokines were relatively high in Ad-tk plus Ad-MCP1 (1:0.01), they were low in Ad-tk plus Ad-MCP1 (1:1). There were almost no differences in the number of macrophages among the tumors treated with various combinations of HSV-tk and MCP-1. Therefore, the types of activated macrophages may be important rather than the numbers recruited and activated. The ratio of IL-12 to IL-10 can be used as a simple metric to classify activated macrophages into two categories, M1 or M2.[23,24] M1 macrophages are potent effector cells that kill microorganisms and tumor cells and produce large amounts of proinflammatory cytokines, particularly IL-12. In contrast, M2 macrophages, a producer of IL-10, tune inflammatory responses and adaptive Th1 immunity, scavenge debris, and promote angiogenesis, tissue remodeling, and repair. The M1/M2 dichotomy of macrophage polarization can elicit both anti- and pro-tumoral activities.[25]

MCP-1 is known to facilitate tumor growth under different conditions, probably by promoting angiogenesis.[8] In the present study, the VEGF expression levels in tumors treated with Ad-tk plus Ad-MCP1 (1:0.1) were low as compared with those treated with Ad-MCP1 alone or Ad-tk plus Ad-MCP1 (1:1 and 1:0.01). A previous study indicated that monocyte recruitment is dependent on the level of MCP-1 secreted by the tumor cells and that the effects of monocyte infiltration on tumor growth are dependent on their levels of infiltration.[26] MCP-1 secreted by apoptotic Huh7 cells may have recruited macrophages more efficiently to these apoptotic cells, thereby resulting in a greater deleterious effect on tumor formation. Therefore, we propose that it is necessary to set the appropriate dosages of the two vectors in the HSV-tk plus MCP-1 system.

Recently, we found that the HSV-tk/GCV system, together with delivery of MCP-1, eradicated HCC and exerted prolonged antitumor effects by activating macrophages and NK cells.[20] In this study, the antitumor immunity increased in mice treated with Ad-tk plus Ad-MCP1 (1:0.1). Several investigators have reported that dying HSV-tk-modified cells released soluble factors, including cytokines.[27,28] These factors could in turn affect the tumor microenvironment, leading to necrosis and inflammation, infiltration of immune cells, up-regulation of costimulatory molecules, and generation of an antitumorigenic immune responses.[28,29] In this immunotherapeutically favorable setting, the optimal dose of MCP-1 with HSV-tk inside the same cell may stimulate tumor-specific immune-mediated cell killing. Consequently, the delivery of an optimal amount of rAd expressing MCP-1 enhanced the antitumor effects of the HSV-tk/GCV system in a model of HCC, and the effects were related to the balance of Th1 and Th2–type cytokines.

References

1 Okada H, Miyamura K, Itoh T *et al.* Gene therapy against an experimental glioma using adeno-associated virus vectors. *Gene Ther* 1996; **3**: 957–64.
2 Coll JL, Mesnil M, Lefebvre MF, Lancon A, Favrot MC. Long-term survival of immunocompetent rats with intraperitoneal colon carcinoma tumors using herpes simplex thymidine kinase/ganciclovir and IL-2 treatments. *Gene Ther* 1997; **4**: 1160–6.
3 Tsuchiyama T, Kaneko S, Nakamoto Y *et al.* Enhanced antitumor effects of a bicistronic adenovirus vector expressing both herpes simplex virus thymidine kinase and monocyte chemoattractant protein-1 against hepatocellular carcinoma. *Cancer Gene Ther* 2003; **10**: 260–9.
4 Kagaya T, Nakamoto Y, Sakai Y *et al.* Monocyte chemoattractant protein-1 gene delivery enhances antitumor effects of herpes simplex virus thymidine kinase/ganciclovir system in a model of colon cancer. *Cancer Gene Ther* 2006; **13**: 357–66.
5 Matsushima K, Larsen CG, DuBois GC, Oppenheim JJ. Purification and characterization of a novel monocyte chemotactic and activating factor produced by a human myelomonocytic cell line. *J Exp Med* 1989; **169**: 1485–90.
6 Rollins BJ, Sunday ME. Suppression of tumor formation *in vivo* by expression of the JE gene in malignant cells. *Mol Cell Biol* 1991; **11**: 3125–31.
7 Nokihara H, Yanagawa H, Nishioka Y *et al.* Natural killer cell-dependent suppression of systemic spread of human lung adenocarcinoma cells by monocyte chemoattractant protein-1 gene transfection in severe combined immunodeficient mice. *Cancer Res* 2000; **60**: 7002–7.
8 Ueno T, Toi M, Saji H *et al.* Significance of macrophage chemoattractant protein-1 in macrophage recruitment, angiogenesis, and survival in human breast cancer. *Clin Cancer Res* 2000; **6**: 3282–9.
9 Mantovani A, Sozzani S, Locati M, Allavena P, Sica A. Macrophage polarization: tumor-associated macrophages as a paradigm for polarized M2 mononuclear phagocytes. *Trends Immunol* 2002; **23**: 549–55.
10 Kijima T, Osaki T, Nishino K *et al.* Application of the Cre recombinase/loxP system further enhances antitumor effects in cell type-specific gene therapy against carcinoembryonic antigen-producing cancer. *Cancer Res* 1999; **59**: 4906–11.
11 Freund CT, Sutton MA, Dang T, Contant CF, Rowley D, Lerner SP. Adenovirus-mediated combination suicide and cytokine gene therapy for bladder cancer. *Anticancer Res* 2000; **20**: 1359–65.
12 Sakai Y, Kaneko S, Sato Y *et al.* Gene therapy for hepatocellular carcinoma using two recombinant adenovirus vectors with alpha-fetoprotein promoter and Cre/lox P system. *J Virol Meth* 2001; **92**: 5–17.
13 Sato Y, Tanaka K, Lee G *et al.* Enhanced and specific gene expression via tissue-specific production of Cre recombinase using adenovirus vector. *Biochem Biophys Res Commun* 1998; **244**: 455–62.
14 Sakai Y, Kaneko S, Nakamoto Y, Kagaya T, Mukaida N, Kobayashi K. Enhanced anti-tumor effects of herpes simplex virus thymidine kinase/ganciclovir system by codelivering monocyte chemoattractant protein-1 in hepatocellular carcinoma. *Cancer Gene Ther* 2001; **8**: 695–704.
15 Kawaguchi T, Suematsu M, Koizumi HM *et al.* Activation of macrophage function by intraperitoneal administration of the streptococcal antitumor agent OK-432. *Immunopharmacology* 1983; **6**: 177–89.
16 Lamont AG, Adorini L. IL-12: a key cytokine in immune regulation. *Immunol Today* 1996; **17**: 214–7.
17 Okamura H, Kashiwamura S, Tsutsui H, Yoshimoto T, Nakanishi K. Regulation of interferon-gamma production by IL-12 and IL-18. *Curr Opin Immunol* 1998; **10**: 259–64.
18 Moore KW, de Waal Malefyt R, Coffman RL, O'Garra A. Interleukin-10 and the interleukin-10 receptor. *Annu Rev Immunol* 2001; **19**: 683–765.
19 Matsukawa A, Lukacs NW, Standiford TJ, Chensue SW, Kunkel SL. Adenoviral-mediated overexpression of monocyte chemoattractant protein-1 differentially alters the development of Th1 and Th2 type responses in vivo. *J Immunol* 2000; **164**: 1699–704.
20 Tsuchiyama T, Nakamoto Y, Sakai Y *et al.* Prolonged, NK cell-mediated antitumor effects of suicide gene therapy combined with monocyte chemoattractant protein-1 against hepatocellular carcinoma. *J Immunol* 2007; **178**: 574–83.
21 Okita K. Management of hepatocellular carcinoma in Japan. *J Gastroenterol* 2006; **41**: 100–6.
22 Mizuguchi H, Xu Z, Ishii-Watabe A, Uchida E, Hayakawa T. IRES-dependent second gene expression is significantly lower than cap-dependent first gene expression in a bicistronic vector. *Mol Ther* 2000; **1**: 376–82.
23 Mantovani A, Sica A, Sozzani S, Allavena P, Vecchi A, Locati M. The chemokine system in diverse forms of macrophage activation and polarization. *Trends Immunol* 2004; **25**: 677–86.
24 Biswas SK, Gangi L, Paul S *et al.* A distinct and unique transcriptional program expressed by tumor-associated macrophages (defective NF-kappaB and enhanced IRF-3/STAT1 activation). *Blood* 2006; **107**: 2112–22.
25 Mantovani A, Bottazzi B, Colotta F, Sozzani S, Ruco L. The origin and function of tumor-associated macrophages. *Immunol Today* 1992; **13**: 265–70.
26 Nesbit M, Schaider H, Miller TH, Herlyn M. Low-level monocyte chemoattractant protein-1 stimulation of monocytes leads to tumor formation in nontumorigenic melanoma cells. *J Immunol* 2001; **166**: 6483–90.
27 Barba D, Hardin J, Sadelain M, Gage FH. Development of anti-tumor immunity following thymidine kinase-mediated killing of experimental brain tumors. *Proc Natl Acad Sci USA* 1994; **91**: 4348–52.
28 Vile RG, Castleden S, Marshall J, Camplejohn R, Upton C, Chong H. Generation of an anti-tumour immune response in a non-immunogenic tumour: HSVtk killing in vivo stimulates a mononuclear cell infiltrate and a Th1-like profile of intratumoural cytokine expression. *Int J Cancer* 1997; **71**: 267–74.
29 Ramesh R, Marrogi AJ, Munshi A, Abboud CN, Freeman SM. *In vivo* analysis of the 'bystander effect': a cytokine cascade. *Exp Hematol* 1996; **24**: 829–38.

doi: 10.1111/j.1349-7006.2008.00951.x

Tumor cell apoptosis induces tumor-specific immunity in a CC chemokine receptor 1- and 5-dependent manner in mice

Noriho Iida,* Yasunari Nakamoto,* Tomohisa Baba,† Kaheita Kakinoki,* Ying-Yi Li,† Yu Wu,† Kouji Matsushima,‡ Shuichi Kaneko,* and Naofumi Mukaida†,[1]

*Disease Control and Homeostasis, Graduate School of Medical Science, and †Division of Molecular Bioregulation, Cancer Research Institute, Kanazawa University, Kanazawa, Japan; and ‡Department of Molecular Preventive Medicine, School of Medicine, University of Tokyo, Tokyo, Japan

Abstract: The first step in the generation of tumor immunity is the migration of dendritic cells (DCs) to the apoptotic tumor, which is presumed to be mediated by various chemokines. To clarify the roles of chemokines, we induced apoptosis using suicide gene therapy and investigated the immune responses following tumor apoptosis. We injected mice with a murine hepatoma cell line, BNL 1ME A.7R.1 (BNL), transfected with HSV-thymidine kinase (tk) gene and then treated the animals with ganciclovir (GCV). GCV treatment induced massive tumor cell apoptosis accompanied with intratumoral DC infiltration. Tumor-infiltrating DCs expressed chemokine receptors CCR1 and CCR5, and T cells and macrophages expressed CCL3, a ligand for CCR1 and CCR5. Moreover, tumor apoptosis increased the numbers of DCs migrating into the draining lymph nodes and eventually generated a specific cytotoxic cell population against BNL cells. Although GCV completely eradicated HSV-tk-transfected BNL cells in CCR1-, CCR5-, or CCL3-deficient mice, intratumoral and intranodal DC infiltration and the subsequent cytotoxicity generation were attenuated in these mice. When parental cells were injected again after complete eradication of primary tumors by GCV treatment, the wild-type mice completely rejected the rechallenged cells, but the deficient mice exhibited impairment in rejection. Thus, we provide definitive evidence indicating that CCR1 and CCR5 and their ligand CCL3 play a crucial role in the regulation of intratumoral DC accumulation and the subsequent establishment of tumor immunity following induction of tumor apoptosis by suicide genes. *J. Leukoc. Biol.* 84: 1001–1010; 2008.

Key Words: *dendritic cells · gene therapy*

INTRODUCTION

Hepatocellular carcinoma (HCC) occurs in individuals with chronic liver disease related to hepatitis B or C virus infections [1–3]. Even after the curative treatments for HCC, such as surgical resection and radiofrequency ablation, tumor recurrence often occurs because of the multicentric development of HCC in the cirrhotic liver [4]. Immune-based therapies, particularly those based on dendritic cells (DCs), may be theoretically effective in preventing the recurrence because of their potential capacity to search for and eradicate tumor cells irrespective of site [5]. However, DC-based therapy is still considered to be in its infancy, probably as a result of the lack of effective techniques for enhancing the immune response to human cancer cells including HCC, which are generally poor in immunogenicity.

Apoptotic tumor cells are generally less immunogenic than necrotic cells, but they can sometimes induce efficient antitumor immune responses depending on the type of apoptosis inducer. Indeed, some anticancer drugs can induce apoptosis of tumor cells and simultaneously enhance the immunogenicity of apoptotic cancer cells [6–8]. Ganciclovir (GCV) can activate the protease family of caspases and induce apoptosis selectively in the cells transfected with the HSV-thymidine kinase (tk) gene [9, 10]. Thus, when GCV is administered systemically to tumor-bearing individuals, it induces apoptosis of HSV-tk-transfected tumor cells but not normal cells. This treatment strategy, designated as suicide gene therapy, can induce immunogenic apoptosis of the tumor cells [11], as evidenced by a massive intratumoral infiltration of macrophages and T cells [12]. Moreover, the expression of various proinflammatory cytokines is augmented at the tumor sites following GCV treatment [12, 13]. Furthermore, to enhance the suicide gene therapy-induced immune responses, the simultaneous use of cytokines such as GM-CSF, IL-2, and MCP-1/CCL2 has been used with some success [14–16]. To design more effective methods of preventing tumor recurrences, it is necessary to fully understand the immune responses after tumor apoptosis induced by HSV-tk/GCV suicide gene therapy.

DCs are potent APC that play a crucial role in the establishment of adoptive immune response. Immature DCs capture and process antigens at the inflammatory sites and thereafter migrate to the draining lymph node, where they

[1] Correspondence: Division of Molecular Bioregulation, Cancer Research Institute, Kanazawa University, 13-1 Takara-machi, Kanazawa 920-0934, Japan. E-mail: naofumim@kenroku.kanazawa-u.ac.jp

Received November 26, 2007; revised June 12, 2008; accepted June 30, 2008.

doi: 10.1189/jlb.1107791

undergo phenotypical and functional maturation. At the draining lymph node, the mature DCs interact with naïve T cells and present the captured and processed antigen to T cells [17, 18].

Chemokines are presumed to play an essential role in the regulation of DC trafficking and DC–T cell interaction in general [19–22]. Circulating immature DCs express inflammatory chemokine receptors such as CCR1, CCR2, CCR5, and CCR6, and these DCs can reach the source of the inflammatory stimulus under the guidance of the ligand gradient for the expressed receptors such as CCL2, CCL3, CCL4, CCL5, CCL7, and CCL20. After capturing antigens, DCs undergo maturation, resulting in a decrease in inflammatory chemokine receptor expression and a reciprocal increase in CCR7 expression. Mature DCs expressing CCR7 migrate to T cell-rich areas of the draining lymph nodes, where the ligands for CCR7, CCL19, and/or CCL21 are expressed abundantly. However, it still remains elusive whether similar mechanisms operate in the DC migration process following massive tumor apoptosis induced by treatments such as gene therapy, chemotherapy, and radiation therapy.

Here, we demonstrate the induction of specific tumor immunity by tumor apoptosis after HSV-tk/GCV suicide gene therapy and essential roles of DCs in this process. Moreover, we provide definitive evidence to indicate that CCR1 and CCR5 and their ligand CCL3 play a key role in the regulation of intratumoral DC accumulation and the subsequent establishment of tumor immunity following induction of tumor apoptosis by HSV-tk/GCV suicide gene therapy. These observations might lay the foundation for devising novel measures to enhance antitumor immune responses to prevent tumor recurrence.

MATERIALS AND METHODS

Mice

Specific pathogen-free, 7- to 9-week-old male BALB/c mice were purchased from Charles River Japan (Yokohama, Japan) and were designated as wild-type (WT) mice. CCL3-deficient [CCL3 knockout (CCL3KO)] mice were obtained from Jackson Laboratories (Bar Harbor, ME, USA). CCR1KO mice were a gift from Dr. Philip M. Murphy [National Institute of Allergy and Infectious Diseases, National Institutes of Health (NIAID, NIH), Bethesda, MD, USA]. CCR5KO mice were generated as described previously [23]. All mice were backcrossed to BALB/c mice for eight to 10 generations. All animal experiments were performed under specific pathogen-free conditions in accordance with the Guideline for the Care and Use of Laboratory Animals of Kanazawa University (Japan).

Tumor cell lines

A murine HCC cell line, BNL 1ME A.7R.1 (BNL), was cultured in DMEM (Sigma Chemical Co., St. Louis, MO, USA) containing 10% FBS (Gibco, Long Island, NY, USA). BNL cells were infected with the retroviral vector pG1Sv.Na harboring HSV-tk cDNA. The infected BNL cells were cultured in 10% FBS-containing DMEM in the presence of 400 μg/ml G418 (Gibco). The surviving cells were tested for sensitivity to GCV in vitro as described previously [24]. GCV-sensitive cells were designated as BNL-tk and were used in the experiments.

Apoptosis detection assay

After culturing for 1 day with 5 μg/ml GCV, BNL-tk cells were harvested, and phosphatidyl serine levels were determined by staining the cells with propidium iodide (PI) and the Annexin V-FITC apoptosis detection kit (Calbiochem, Darmstadt, Germany) according to the manufacturer's instructions. At least 50,000 stained cells were analyzed on a FACSCalibur system (BD Biosciences, San Diego, CA, USA) for each determination.

Tumor injection

Seven- to 9-week old male WT, CCR1KO, CCR5KO, and CCL3KO mice were inoculated s.c. into the left flank with 2×10^5 BNL-tk cells on Day 0. From Days 14 to 18 (5 consecutive days), 75 mg/kg GCV (i.p.) was administered daily (see **Fig. 1C**). Tumors were removed at the indicated time intervals for immunohistochemical analysis and quantitative real-time RT-PCR. In another series of experiments, WT, CCR1KO, CCR5KO, or CCL3KO mice were inoculated with 1.5×10^5 BNL-tk on Day 0. The mice were i.p.-injected with 75 mg/kg GCV from Days 2 to 5. The animals were then rechallenged s.c. with 1.0×10^5 BNL in their right flank on Day 18, after confirming that the primary tumors were eradicated completely (see Fig. 5A). Tumor sizes were evaluated twice each week using calipers, and tumor volume was calculated by the following formula: Tumor volume (mm^3) = (the longest diameter) × (the shortest diameter)^2/2.

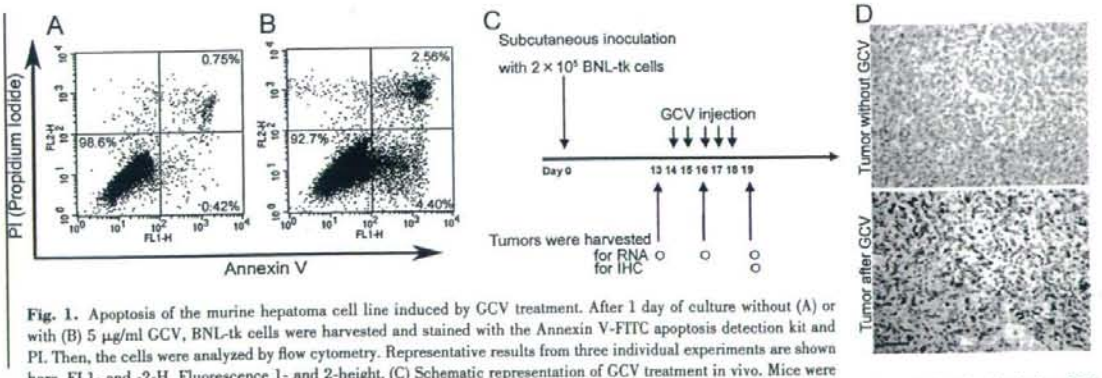

Fig. 1. Apoptosis of the murine hepatoma cell line induced by GCV treatment. After 1 day of culture without (A) or with (B) 5 μg/ml GCV, BNL-tk cells were harvested and stained with the Annexin V-FITC apoptosis detection kit and PI. Then, the cells were analyzed by flow cytometry. Representative results from three individual experiments are shown here. FL1- and -2-H, Fluorescence 1- and 2-height. (C) Schematic representation of GCV treatment in vivo. Mice were s.c.-injected with 2×10^5 BNL-tk cells on Day 0. Then, GCV was i.p.-injected into mice from Days 14 to 18. Tumors were harvested on the day before GCV injection (Day 13), on Day 3 or 6 after GCV injection (Day 16 or 19) for real-time RT-PCR analysis, and on Day 19 for immunohistochemistry (IHC). (D) Apoptotic cells detected in tumor tissues with or without GCV treatment using anti-ssDNA antibody. Original magnification, ×400. Original bar, 50 μm.

The draining lymph nodes (inguinal and axillary) were removed from the mice at the indicated time intervals for flow cytometric analysis and cytotoxicity assay.

Immunohistochemical analysis

Rabbit anti-mouse CCR5 polyclonal antibodies were prepared as described previously [25]. The removed tumor tissues were embedded in paraffin or the Sakura Tissue-Tek OCT compound (Sakura Finetek, Torrance, CA, USA) as frozen tissues. The paraffin-embedded sections were then stained with goat anti-mouse CCR1 (Santa Cruz Biotechnology, Santa Cruz, CA, USA), rabbit anti-CCR5, goat anti-mouse CCL3 (R&D Systems, Minneapolis, MN, USA), rat anti-mouse F4/80, anti-mouse CD3 (Serotec, Oxford, UK), rabbit anti-ssDNA, or rat anti-Ki67 (Dako Cytomation, Tokyo, Japan) overnight at 4°C. Cryostat sections of the frozen tissues were fixed with 4% paraformaldehyde (PFA) in PBS and stained with rat anti-mouse DEC205 (Serotec) or hamster anti-mouse CD11c (BD Biosciences) overnight at 4°C. The sections were then incubated for 1 h at room temperature with biotinylated rabbit anti-goat IgG, biotinylated swine anti-rabbit IgG, biotinylated rabbit anti-rat IgG (Dako Cytomation), or biotinylated mouse anti-hamster IgG (BD Biosciences). The immune complexes were visualized using a catalyzed signal amplification system (Dako Cytomation) or the ELITE avidin-biotin-peroxidase and diaminobenzidine substrate kits (Vector Laboratories, Burlingame, CA, USA), except for anti-ssDNA, where a novel HRP-labeled polymer (Envision$^+$, Dako Cytomation) was used, according to the manufacturer's instructions. As a negative control, goat IgG (R&D Systems), rabbit IgG (Dako Cytomation), rat IgG (Cosmo Bio, Tokyo, Japan), or hamster IgG (BD Biosciences) was used instead of specific primary antibodies. The numbers of positive cells were determined in each animal in 10 randomly chosen fields at 400-fold magnification by an examiner without any prior knowledge of the experimental procedures.

Double-color immunofluorescence analysis

Tumor tissues were embedded in paraffin or the OCT compound as frozen tissues. The paraffin-embedded sections were then stained with combinations of rat anti-mouse CD3 and goat anti-mouse CCL3 or anti-F4/80 and anti-CCL3 antibodies overnight at 4°C. After fixation with 4% PFA/PBS, cryostat sections were stained with the combinations rat anti-mouse CD4 (BD Biosciences) and anti-CCR1, rat anti-mouse CD8a (BD Biosciences) and anti-CCR1, anti-CD4 and anti-CCR5, anti-CD8a and anti-CCR5, rat anti-DEC205 and anti-CCR1, anti-DEC205 and anti-CCR5, PE-conjugated hamster anti-CD11c (BD Biosciences) and anti-CCR1, PE-conjugated anti-CD11c and anti-CCR5, PE-conjugated anti-CD11c and rat anti-CD11b (BD Biosciences), or PE-conjugated anti-CD11c and anti CD8a antibodies. After extensive washing, AF488 donkey anti-rat IgG (Invitrogen, Carlsbad, CA, USA) was applied as the secondary antibody to detect CD4-, CD8a-, CD3-, F4/80-, DEC205-, or CD11b-positive cells. Simultaneously, AF546 or AF488 donkey anti-goat IgG (Invitrogen) was used to detect CCR1- or CCL3-positive cells, and AF594 or AF488 donkey anti-rabbit IgG (Invitrogen) was used to detect CCR5-positive cells. The sections were observed using a confocal microscope (LSM 510 META, Zeiss, Thornwood, NY, USA). The percentage of double-positive cells was determined in each animal in five randomly chosen fields at 400-fold magnification by an examiner without any prior knowledge of the experimental procedures.

Flow cytometric analysis

Inguinal and axillary lymph nodes were removed and digested in a DNase I and collagenase solution (Sigma Chemical Co.). The resultant, single-cell preparations were stained with various combinations of FITC-labeled anti-CD4, FITC-labeled anti-CD86, PE-labeled anti-CD8, PE-labeled anti-CD11c, PE-labeled anti-CD44, and PE-labeled anti-CD62 ligand (CD62L) mAb (BD Biosciences). FITC-rat IgG, PE-hamster IgG, and PE-rat IgG were used as isotype controls (BD Biosciences). To prepare the tumor lysate, BNL or CT26 cells were suspended in PBS and subjected to four cycles of rapid freezing in liquid nitrogen and thawing at 55°C. The lysate was spun at 15,000 rpm to remove particulate cellular debris. To stain intracellular IFN-γ, the mononuclear cells harvested from the draining lymph nodes on Day 8 (see Fig. 5A) were incubated with the BNL or CT26 lysates at a tumor cell:mononuclear cell ratio of 1:1 in the presence of GolgiPlug (BD Biosciences). Six hours later, surface staining was performed with APC-conjugated CD8 antibodies. Intracellular IFN-γ was stained after fixation and permeabilization with BD Cytofix/Cytoperm buffer with PE-conjugated IFN-γ antibodies or isotype control using the Mouse Intracellular Cytokine Staining starter kit (BD Biosciences). At least 100,000 stained cells were analyzed on a FACSCalibur system for each determination. The data were expressed as a proportion of positive cells (compared with cells stained with an irrelevant control antibody), and the absolute positive cell numbers were calculated after determining the total cell numbers in the lymph nodes by the following formula: Absolute positive cell numbers = total cell number in the lymph nodes × percentage of positive cells × 1/100.

Quantitative real-time RT-PCR

Total RNA was extracted from the resected tumor and lymph nodes using RNA-Bee (Tel-Test, Friendswoods, TX, USA), according to the manufacturer's instructions. After the RNA preparations were further treated with RNase-free DNase I (Life Technologies, Gaithersburg, MD, USA) to remove residual DNA, cDNA was synthesized as described previously [26]. Quantitative real-time PCR was performed on an Applied Biosystems StepOne™ real-time PCR system (Applied Biosystems, Foster City, CA, USA) using the comparative threshold (C_T) quantification method. TaqMan® gene expression assays (Applied Biosystems) containing specific primers (Accession Numbers CCL3, Mm00441258_ml; CCL4, Mm00443111_m1; CCL5, Mm01302428_ml; CCR1, Mm00438260_s1; CCR5, Mm01216171_m1; GAPDH, Mm99999915_g1), TaqMan® minor groove binder probe (FAM™ dye-labeled), and TaqMan® fast universal PCR master mix were used with 10 ng cDNA to detect and quantify the expression levels of CCL3, CCL4, CCL5, CCR1, and CCR5. Reactions were performed for 20 s at 95°C and then for 40 cycles of 1 s at 95°C and 20 s at 60°C. GAPDH was amplified as an internal control. C_T values of GAPDH were subtracted from C_T values of the target genes (ΔC_T). ΔC_T values of tumors after GCV injection were compared with ΔC_T values of tumors before GCV injection.

Cytotoxicity assay

Mononuclear cells were isolated from the draining lymph nodes at the indicated time intervals and were incubated at a cell density of 2×10^6 cells/ml in the presence of 0.6×10^6 cells/ml BNL cells, which were irradiated at 50 Gy beforehand. After 5 days of culture, the cells were tested for cytotoxicity in a lactate dehydrogenase assay using the CytoTox 96 nonradioactive cytotoxicity assay kit (Promega, Madison, WI, USA), according to the manufacturer's instructions. Effector cells were added to target cells in triplicate at different E:T ratios. Percentage of specific lysis was calculated using the following formula: [(experimental−effector spontaneous−target spontaneous)/(target maximum−target spontaneous)] × 100%.

Adoptive transfer of DC

Draining lymph nodes were harvested on Day 8 (see Fig. 5A) and were digested with DNase I and collagenase solution. Mononuclear cells were obtained by centrifugation over a Histopaque-1077 density gradient (Sigma Chemical Co.), and DCs were isolated by CD11c-conjugated magnetic microbeads (Miltenyi Biotec, Auburn, CA, USA). CD11c-positive DCs (2.5×10^5/mouse) were injected into the left flank of GCV-treated KO mice on Day 8 (see Fig. 5A). On Day 18, DC-transferred mice were rechallenged with 1×10^5 BNL cells in their right flank, and tumor sizes were measured.

Statistical analysis

Data were analyzed statistically using one-way ANOVA followed by the Tukey-Kramer test, except for tumor progression data, which were analyzed using two-way ANOVA. Data of tumor sizes after adoptive transfer of the DC experiment were analyzed using the Mann-Whitney U test. $P < 0.05$ was considered statistically significant.

RESULTS

GCV treatment induces tumor cell apoptosis with intratumoral CCR1-, CCR5-, and CCL3-positive cell accumulation in WT mice

We investigated whether HSV-tk-GCV treatment can induce apoptosis in vitro in the tk-transfected murine hepatoma cell line BNL-tk. GCV treatment significantly increased the proportions of early (annexin-positive but PI-negative) and late (annexin-positive and PI-positive) apoptotic cells (Fig. 1, A and B). We injected GCV into WT mice i.p. after the s.c. BNL-tk tumor was formed macroscopically, according to the schedule, as shown in Figure 1C. Microscopic analysis revealed that more than half of the tumor cells were apoptotic and that a large number of mononuclear cells had accumulated in the tumor sites on Day 19 immediately following the completion of treatment (Fig. 1D and Supplemental Fig. 1). Thereafter, the tumor regressed macroscopically. We next investigated the chemokine receptor expression by tumor-infiltrating cells after the induction of in vivo tumor apoptosis by suicide gene therapy. Immunohistochemical analysis revealed the presence of few CCR1-, CCR5-, or CCL3-positive cells in tumors without GCV treatment (**Fig. 2A**). In contrast, GCV treatment caused intratumoral infiltration of a large number of CCR1-, CCR5-, and CCL3-positive cells in WT mice, along with massive apoptosis of tumor cells (Fig. 2A and Supplemental Fig. 2). The intratumoral mRNA expression of CCL3, CCL4, and CCL5 was markedly increased 3 days after GCV treatment, whereas that of their receptors CCR1 and CCR5 was augmented later than 3 days after GCV injection (Fig. 2B).

Tumor-infiltrating DCs express CCR1 and CCR5

To determine the type of tumor-infiltrating cells expressing CCR1, CCR5, or CCL3, we performed a double-color immunofluorescence analysis. CD4- and CD8-positive T cells expressed CCR5 but not CCR1 (**Fig. 3A** and Supplemental Fig. 3A; 78.2±8.9% of CD4-positive T cells and 92.6±8.2% of CD8-positive T cells expressed CCR5, and CCR1 was not detected in CD4- or CD8-positive T cells). In contrast, CD11c- and DEC205-positive cells, which infiltrated to tumor sites of WT mice after GCV treatment, expressed CCR1 and CCR5 (Fig. 3B and Supplemental Fig. 3B; 100% of CD11c-positive DCs expressed CCR1 and CCR5, 97.5±5.6% DEC205-positive cells expressed CCR1, and 100% DEC-positive cells expressed CCR5). Moreover, tumor-infiltrating, CD11c-positive DCs exhibited a "myeloid" phenotype, as 87.8 ± 14.8% of CD11c-positive cells expressed CD11b, and none of them expressed CD8a (Supplemental Fig. 3C). Furthermore, CCL3 proteins were detected in CD3-positive T cells, F4/80-positive macrophages (Fig. 3C; 72.0±9.1% of CD3-positive T cells and 87.0±12.0% of F4/80-positive macrophages expressed CCL3). These observations suggest that apoptosis induced by GCV treatment enhanced the expression of CCL3, CCL4, and CCL5 and then produced chemokines attracted to CD11c-positive DCs as well as CD3-positive T cells. To address this possibility, we investigated intratumoral infiltration of CD11c-positive DCs and CD3-positive T cells in CCR1KO, CCR5KO, or CCL3KO mice, which were s.c.-inoculated with 2×10^5 BNL-tk cells into WT and KO mice. The lack of CCR1, CCR5, or CCL3 had no discernible effects on the growth of primary tumors (**Fig. 4A**). Then, we injected GCV i.p. into the mice as shown in Figure 1C. Immunohistochemical analysis revealed

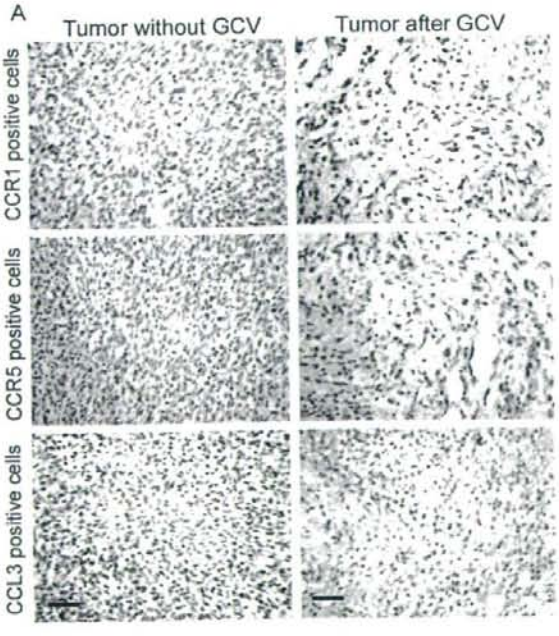

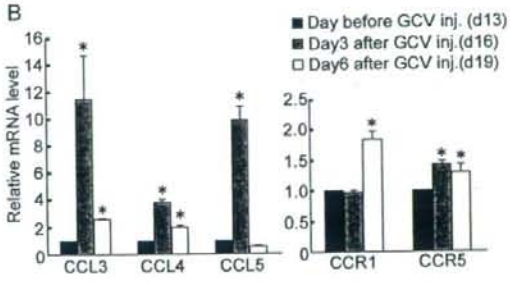

Fig. 2. Accumulation of tumor-infiltrating CCR1-, CCR5-, or CCL3-positive cells after tumor apoptosis induced by GCV treatment. Mice were inoculated with BNL-tk cells according to the schedule shown in Figure 1C. (A) Tumors were removed from WT mice on Day 19, and immunohistochemical analysis was performed using anti-CCR1, -CCR5, or -CCL3 antibody on tumors with or without GCV treatment. Representative results from three individual animals in each group are shown here. Original magnification, ×400. Original bars, 50 μm. (B) Real-time RT-PCR was performed on total RNA extracted from the tumor of WT mice harvested on Days 13, 16, or 19. The level of chemokine mRNA was normalized to GAPDH mRNA levels. Bars, ±1 SD ($n=3$); *, $P < 0.05$, compared with the day before GCV injection.

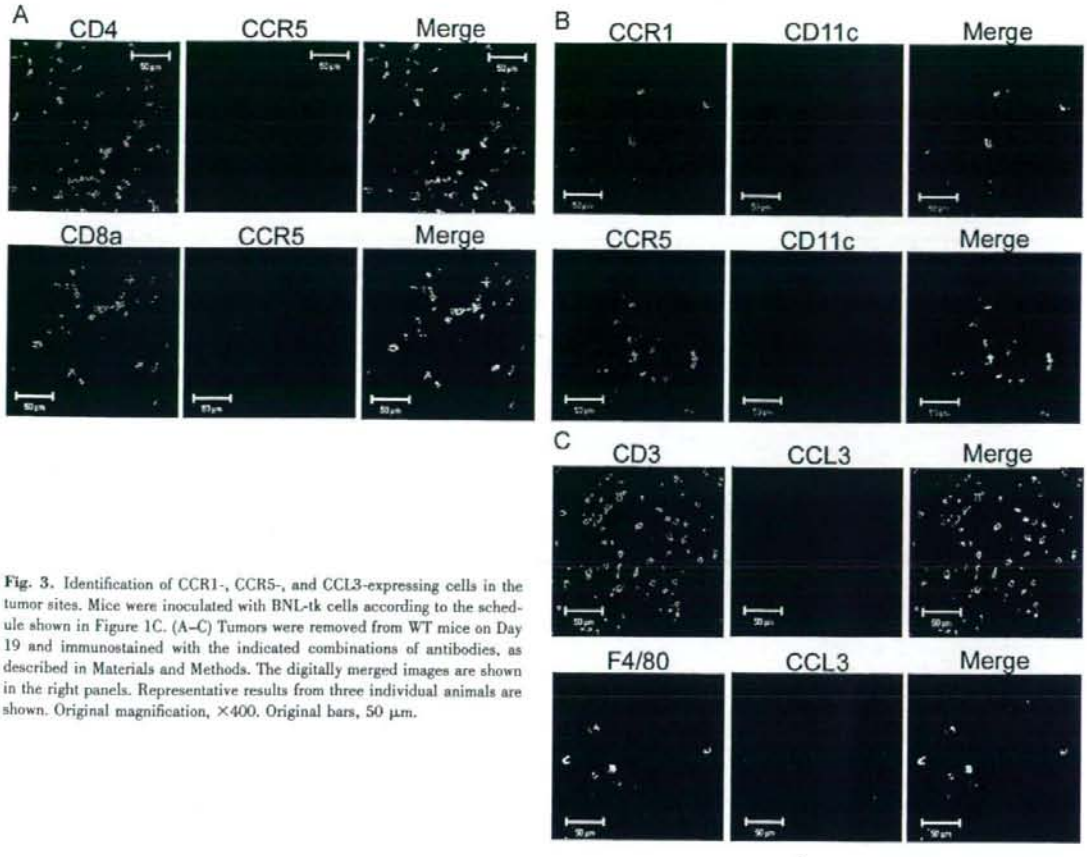

Fig. 3. Identification of CCR1-, CCR5-, and CCL3-expressing cells in the tumor sites. Mice were inoculated with BNL-tk cells according to the schedule shown in Figure 1C. (A–C) Tumors were removed from WT mice on Day 19 and immunostained with the indicated combinations of antibodies, as described in Materials and Methods. The digitally merged images are shown in the right panels. Representative results from three individual animals are shown. Original magnification, ×400. Original bars, 50 μm.

the presence of few CD3-, F4/80-, or DEC205-positive cells in tumors without GCV treatment (Fig. 4B). GCV treatment induced tumor cell apoptosis in CCL3KO, CCR1KO, and CCR5KO mice to a similar extent as that in WT mice (data not shown). Moreover, GCV treatment caused intratumoral accumulation of a large number of CD3-, CD4-, and CD8-positive T cells and DEC205- and CD11c-positive DCs in WT mice (Fig. 4, B and C). By contrast, the increases in intratumorally accumulating DEC205- and CD11c-positive cells and to a lesser extent, CD3-, CD4-, and CD8-positive cells were attenuated in CCR1KO, CCR5KO, and CCL3KO mice (Fig. 4, B and C). In contrast, GCV treatment induced intratumoral infiltration of F4/80-positive macrophages (Fig. 4B) and CD49b/DX5-positive NK cells (data not shown) in WT and KO mice to a similar extent.

Partial failure of CCR1KO, CCR5KO, and CCL3KO mice in rejecting the rechallenged tumor

Apoptosis induced by GCV treatment caused intratumoral infiltration of DCs and T cells in a CCR1- and/or CCR5-dependent manner. As intratumoral infiltration of DCs and T cells is a prerequisite for the establishment of specific tumor immunity, we examined the immune status of GCV-treated mice by rechallenging the parental BNL cell line. To completely eradicate the primary BNL-tk tumor, GCV was administered between 2 and 5 days after the tumor injection (**Fig. 5A**). Primary BNL-tk tumors were eradicated completely in WT, CCR1KO, CCR5KO, and CCL3KO mice at similar rates (data not shown). When these mice were injected again with parental BNL cells, WT mice rejected them completely. In contrast, CCR1KO, CCR5KO, and CCL3KO mice failed to completely eliminate the rechallenged tumor cells, although the growth rates were retarded in these mice compared with naïve WT mice (Fig. 5B). A marked cytotoxicity against BNL but not in CT26 cells was observed when draining lymph node-derived mononuclear cells of GCV-treated WT mice were used as effector cells. Only a modest amount of cytotoxicity was detected when mononuclear cells in the draining lymph nodes of GCV-treated CCR1KO, CCR5KO, or CCL3KO mice were used as effector cells (Fig. 5C). Further, GCV-induced tumor apoptosis enhanced the mRNA expression of Th1 cytokines such as IFN-γ, IL-12p40, and IL-18 in the draining lymph nodes of WT mice but not of CCR1KO, CCR5KO, and CCL3KO mice (Supplemental Fig. 4). Likewise, $CD8^+IFN\text{-}\gamma^+$ cells were increased markedly in GCV-treated WT mice when lymph node-derived mononuclear cells were cocultured with BNL cell lysates, compared with tumor-bearing or tumor-free

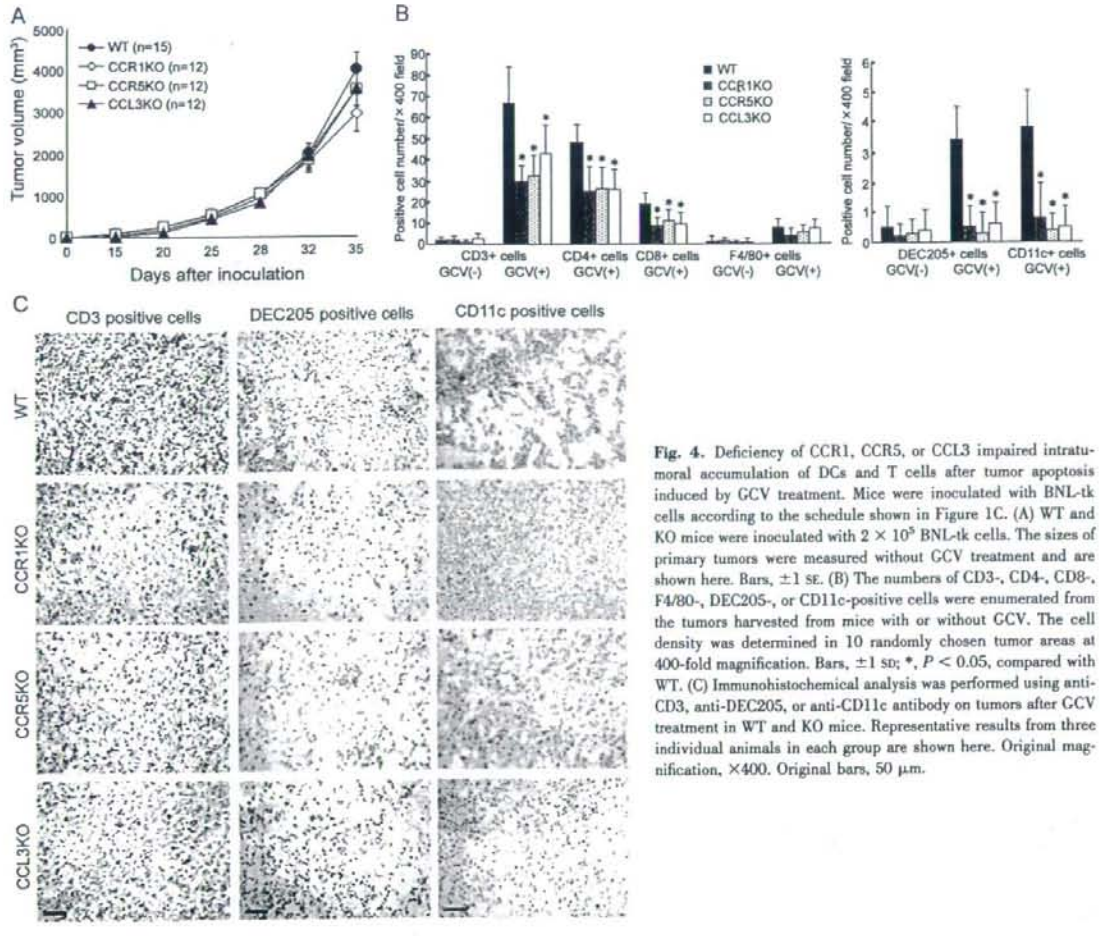

Fig. 4. Deficiency of CCR1, CCR5, or CCL3 impaired intratumoral accumulation of DCs and T cells after tumor apoptosis induced by GCV treatment. Mice were inoculated with BNL-tk cells according to the schedule shown in Figure 1C. (A) WT and KO mice were inoculated with 2×10^5 BNL-tk cells. The sizes of primary tumors were measured without GCV treatment and are shown here. Bars, ±1 SE. (B) The numbers of CD3-, CD4-, CD8-, F4/80-, DEC205-, or CD11c-positive cells were enumerated from the tumors harvested from mice with or without GCV. The cell density was determined in 10 randomly chosen tumor areas at 400-fold magnification. Bars, ±1 SD; *, $P < 0.05$, compared with WT. (C) Immunohistochemical analysis was performed using anti-CD3, anti-DEC205, or anti-CD11c antibody on tumors after GCV treatment in WT and KO mice. Representative results from three individual animals in each group are shown here. Original magnification, ×400. Original bars, 50 μm.

WT mice (Fig. 5D). Increases in $CD8^+IFN\text{-}\gamma^+$ cells were less evident in CCR1KO, CCR5KO, or CCL3KO mice treated with tumor cells and GCV compared with WT mice when lymph node-derived cells were cocultured with BNL cell lysates (Fig. 5D). These observations suggest that the absence of CCR1, CCR5, or CCL3 greatly impaired the apoptosis-induced establishment of specific tumor immunity.

Apoptosis-induced migration of DCs to draining lymph nodes and intranodal T cell proliferation activation in a CCR1-, CCR5-, and/or CCL3-dependent manner

Tumor-infiltrating DCs can uptake tumor antigens at the tumor sites and migrate to the draining lymph nodes, where they mature to present antigens to T cells [17, 18]. Thus, we further explored the status of DCs as well as T cells in the draining lymph nodes. Following GCV treatment, tumor apoptosis increased the proportions of $CD86^+CD11c^+$ cells in the draining lymph nodes but not in distant lymph nodes in WT mice (**Fig. 6A**). In contrast, GCV-induced increases in $CD11c^+$ cell proportion were depressed in CCR1KO, CCR5KO, or CCL3KO mice (Fig. 6A). The levels of CD86 on $CD11c^+$ cells were increased in GCV-treated WT mice compared with WT mice, which had been injected with neither BNL-tk cells nor GCV, although the levels of CD86 were depressed in the KO mice (mean fluorescent intensities of CD86 on $CD11c^+$ cells: WT/BNL-tk/GCV, 114.3±8.6; WT/BNL-tk, 86.2±12.2; WT/no tumor, 86.5±2.6; CCR1KO/BNL-tk/GCV, 85.4±15.6; CCR5KO/BNL-tk/GCV, 92.3±12.6; CCL3KO/BNL-tk/GCV, 79.0±9.8). Moreover, GCV-induced tumor apoptosis significantly increased the numbers of total cells, $CD4^+$ and $CD8^+$ cells, in the draining lymph nodes of WT mice. GCV-induced increases in these cell populations were also attenuated in CCR1KO, CCR5KO, or CCL3KO mice (Fig. 6B). Lymphocytes expressing the cell proliferation marker Ki67 were increased in the paracortical areas of the draining lymph nodes of GCV-treated WT mice compared with the other groups (Fig. 6C and Supplemental Fig. 5). Injection of BNL-tk cells marginally increased the proportion of activated $CD4^+$ T cells, defined as $CD44^{hi}CD62L^{lo}CD4^+$, in the draining lymph nodes. Coinjec-

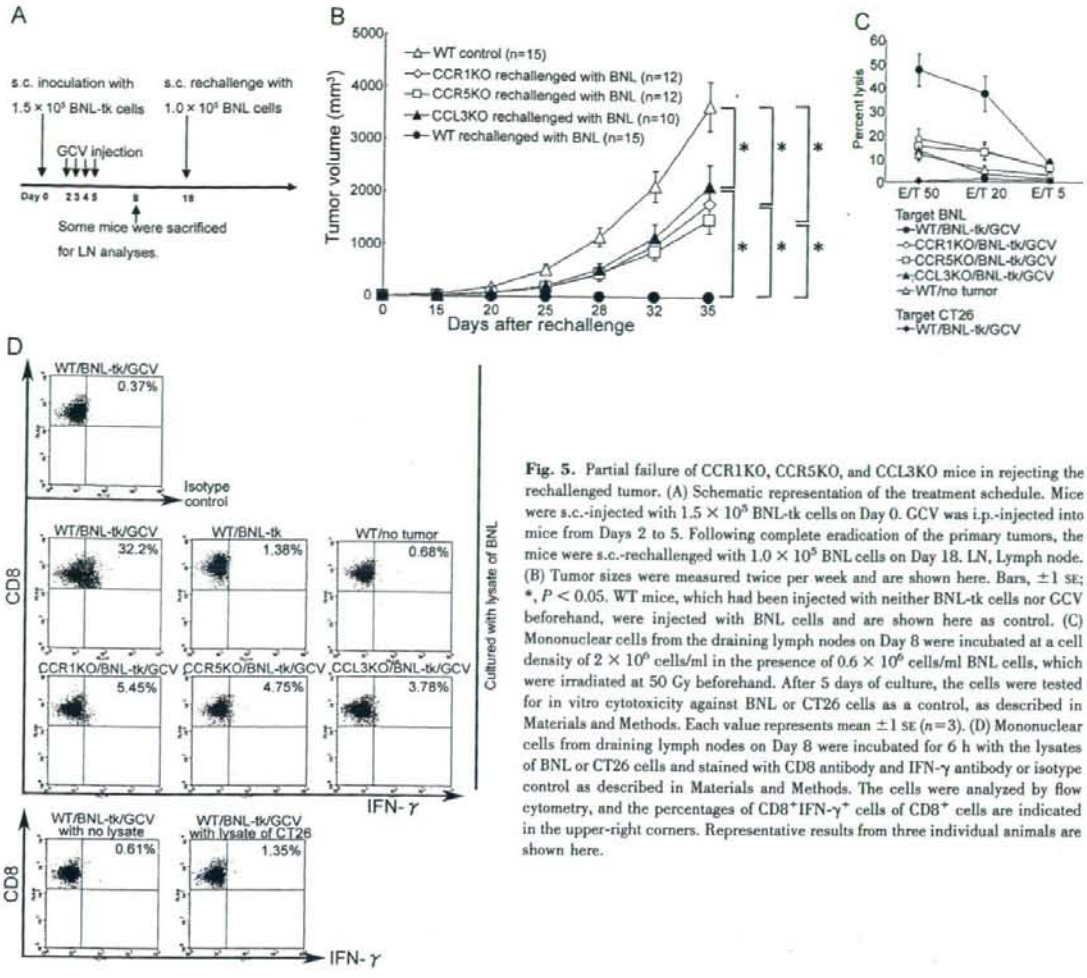

Fig. 5. Partial failure of CCR1KO, CCR5KO, and CCL3KO mice in rejecting the rechallenged tumor. (A) Schematic representation of the treatment schedule. Mice were s.c.-injected with 1.5×10^5 BNL-tk cells on Day 0. GCV was i.p.-injected into mice from Days 2 to 5. Following complete eradication of the primary tumors, the mice were s.c.-rechallenged with 1.0×10^5 BNL cells on Day 18. LN, Lymph node. (B) Tumor sizes were measured twice per week and are shown here. Bars, ±1 SE; *, $P < 0.05$. WT mice, which had been injected with neither BNL-tk cells nor GCV beforehand, were injected with BNL cells and are shown here as control. (C) Mononuclear cells from the draining lymph nodes on Day 8 were incubated at a cell density of 2×10^6 cells/ml in the presence of 0.6×10^6 cells/ml BNL cells, which were irradiated at 50 Gy beforehand. After 5 days of culture, the cells were tested for in vitro cytotoxicity against BNL or CT26 cells as a control, as described in Materials and Methods. Each value represents mean ±1 SE ($n=3$). (D) Mononuclear cells from draining lymph nodes on Day 8 were incubated for 6 h with the lysates of BNL or CT26 cells and stained with CD8 antibody and IFN-γ antibody or isotype control as described in Materials and Methods. The cells were analyzed by flow cytometry, and the percentages of $CD8^+IFN\text{-}\gamma^+$ cells of $CD8^+$ cells are indicated in the upper-right corners. Representative results from three individual animals are shown here.

tion of GCV further augmented this increment in WT mice but not in KO mice (Fig. 6, D and E). These observations suggest that the absence of CCR1, CCR5, or CCL3 impaired the GCV-induced migration of DCs into the draining lymph nodes and the subsequent proliferation and activation of T cells in the draining lymph nodes.

Restoration of anti-tumor response of KO mice by adoptive transfer of DCs harvested from GCV-treated WT mice

Given the proposed, crucial role of DCs in evoking antitumor immunity after tumor apoptosis, we finally performed adoptive transfer of DCs harvested from the draining lymph nodes of GCV-treated WT mice into the KO mice. DCs were harvested from the draining lymph nodes of GCV-treated, tumor-bearing or tumor-free WT mice and were transferred s.c. into the KO mice on Day 8 (Fig. 5A). The KO mice completely rejected the rechallenged cells when DCs were transferred from GCV-treated, tumor-bearing WT mice but not tumor-free WT mice (**Fig. 7**). These observations suggest that GCV-induced tumor apoptosis mediated the trafficking of DCs to the draining lymph nodes, which can induce the establishment of specific immunity in a CCR1-, CCR5-, or CCL3-dependent manner.

DISCUSSION

Apoptosis was previously presumed to be immunologically silent or even tolerogenic [27]. However, recent reports have indicated that tumor cell apoptosis can induce antitumor immune responses effectively, as the immunogenicity of apoptotic tumor cells is dependent on apoptosis inducers. Indeed, gemcitabine-induced apoptosis can augment cross-priming of tumor-specific $CD8^+$ T cells in vivo rather than cross-tolerizing [8]. Similarly, apoptosis induced by local radiation therapy can generate tumor antigen-specific effector cells that migrate to

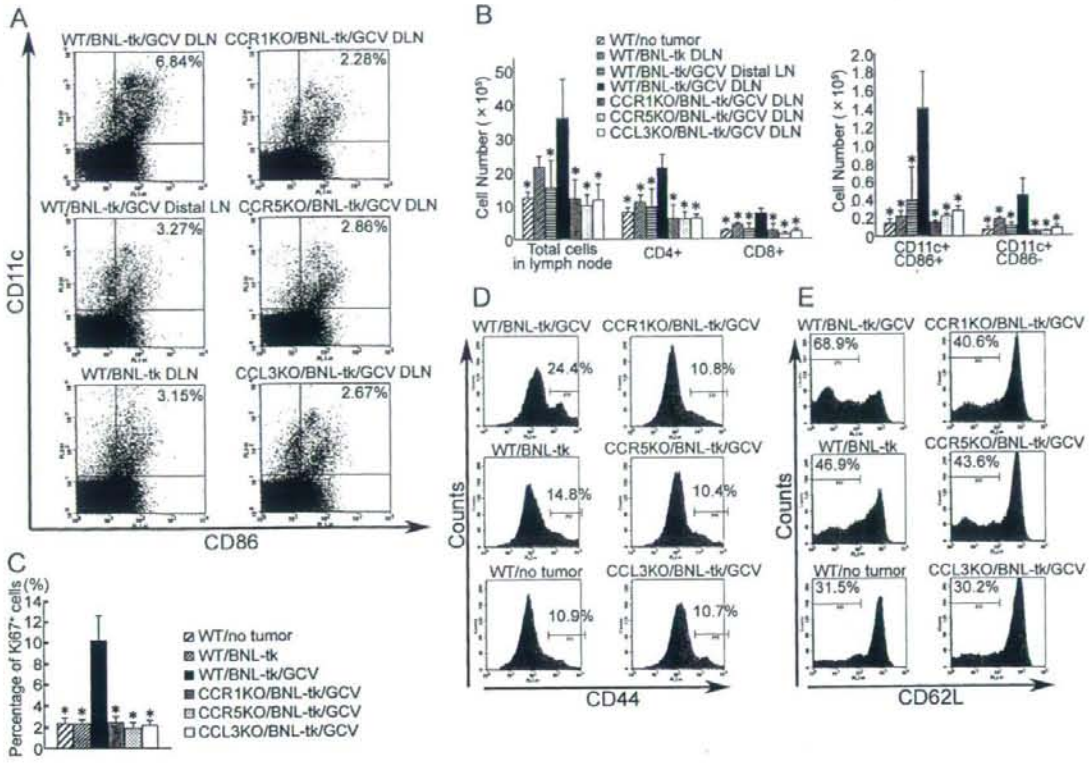

Fig. 6. Apoptosis-induced migration of DCs to the draining lymph nodes (DLN) and intranodal T cell proliferation and activation in a CCR1-, CCR5-, and/or CCL3-dependent manner. Mice were treated according to the schedule shown in Figure 5A. (A) Draining lymph nodes or distal lymph nodes were harvested on Day 8 as indicated in Figure 5A. Mononuclear cells were stained with a combination of FITC-labeled anti-CD86 and PE-labeled anti-CD11c antibodies. The percentage of $CD11c^+CD86^+$ cells was determined and is indicated in the upper-right corners. Representative results from three individual animals are shown here. (B) Absolute cell numbers of each cell population in the draining lymph nodes or distal lymph nodes on Day 8 were determined as described in Materials and Methods. Error bars, ±1 SD; *, $P < 0.05$, compared with draining lymph nodes derived from WT mice treated with BNL-tk/GCV. (C) Draining lymph nodes harvested on Day 8 were immunostained with anti-Ki67 antibody, and percentages of $Ki67^+$ cells in lymph nodes were determined. Error bars, ±1 SD; *, $P < 0.05$, compared with draining lymph nodes derived from WT mice treated with BNL-tk/GCV. (D and E) Mononuclear cells harvested on Day 8 were stained with a combination of FITC-labeled anti-CD4 and PE-labeled anti-CD44 (D) or PE-labeled anti-CD62L (E) antibodies. Histograms were gated on CD4-positive cells, and percentages of $CD44^{hi}$ (D) or $CD62L^{lo}$ (E) cells were determined. Representative results from three individual animals are shown here.

the tumor [28]. Moreover, apoptotic change caused by anthracyclin can induce the translocation of calreticulin to the apoptotic tumor cell surface, and calreticulin exposure can enhance the immunogenicity of apoptotic cancer cells [6, 7]. Thus, apoptosis induced by these measures is sufficiently immunogenic to prevent tumor progression.

The combination of HSV-tk gene transfer and GCV can efficiently induce the apoptosis of the transfected tumors as observed in the present study. Here, we also observed that the treatment augmented the immune response, as evidenced by an increase in the number of tumor-infiltrating DCs. Subsequently, the number of DCs in the draining lymph nodes increased together with enhanced, specific immunity to the injected tumor. These observations suggest that tumor apoptosis induced by HSV-tk/GCV treatment is effective in generating specific tumor immunity, similar to that observed in the case of anticancer drug treatment.

Consistent with our present observations, CCL3 and its related chemokine CCL5 were detected in macrophages infiltrating human cancer tissues [29, 30]. Given their potent chemotactic activity against various types of immune cells [31], gene transfer of CCL3 or CCL5 induced the accumulation of immune cells including DCs, T cells, macrophages, and NK cells in the tumor sites, resulting in delayed tumor growth and prolonged survival [16, 32–34]. Moreover, combination therapy of the HSV-tk and CCL3/CCL20 gene induces an exaggerated accumulation of DCs, $CD4^+$ cells, $CD8^+$ cells, NK cells, and macrophages in the tumor sites compared with HSV-tk/GCV treatment alone, and the net effects are tumor regression and prolonged survival [34]. However, the roles of endogenously produced CCL3 and its related chemokines in tumor apoptosis still remain to be elucidated.

In human HCC, tumor-infiltrating lymphocytes express high levels of CCR5 and CXCR3. Moreover, these lymphocytes

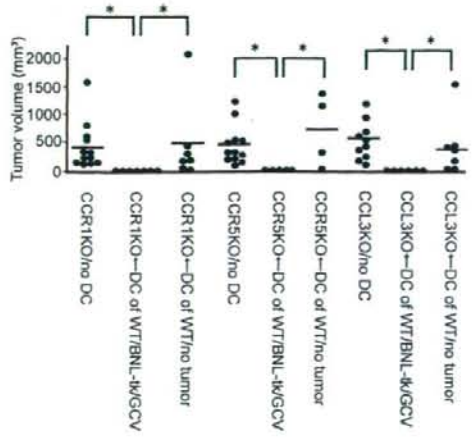

Fig. 7. Adoptive transfer of DCs harvested from GCV-treated WT mice restored the antitumor response of KO mice. After inoculation of BNL-tk tumors, CCR1KO, CCR5KO, or CCL3KO mice were treated with GCV from Days 2 to 5 as described in Figure 5A. The DCs were then harvested from the draining lymph nodes of GCV-treated WT mice and transferred s.c. into the KO mice on Day 8 as shown in Figure 5A. On Day 18, these mice were injected again with parental BNL cells, and tumor sizes were measured on Day 28. GCV-treated KO mice, transferred without or with DCs of naïve WT mice, were also rechallenged with parental BNL cells as control. Bars, mean; *, $P < 0.05$.

show strong chemotactic responses to CC and CXC chemokines including CCL3, CCL4, and CXCL9 [35]. Additional treatments are nevertheless required to enhance the immune responses, as the CCR5- or CXCR3-positive lymphocytes are insufficient to evoke immune responses and eradicate tumor tissues. We demonstrated that suicide gene therapy-induced tumor cell apoptosis augments CCR1- and CCR5-positive cell infiltration into the hepatoma tissues. Further, these CCR1- or CCR5-positive cells are DCs and/or T cells—the cells indispensable for tumor immunity. Thus, suicide gene therapy can potentially enhance tumor immunity by attracting these immune cells to the apoptotic tumor cells.

The initial step leading to specific tumor immunity is the capture of tumor antigens by macrophages and immature DCs, both of which accumulate in tumor sites. However, in this model, CCR1KO, CCR5KO, and CCL3KO mice failed to completely eliminate the rechallenged tumor cells along with reduced intratumoral accumulation of DCs but not F4/80-positive macrophages. These observations suggest that the establishment of specific tumor immunity requires intratumoral recruitment of immature DCs but not macrophages. Activated NK cells can also induce DC maturation in lymphoid organs as well as in nonlymphoid tissues. Although NK cells express chemokine receptors such as CCR5 [36], the deficiency of CCR1 or CCR5 has little effects on intratumoral infiltration of NK cells. These observations preclude the crucial role of NK cells in the establishment of specific tumor immunity in this model.

Immature DCs use several chemokine receptors including CCR1, CCR2, CCR4, CCR5, CCR6, CCR8, and CXCR4 for their migration [22]. However, the chemokine receptor(s) regulating immature DC trafficking to tumor sites still need(s) to be determined. We previously observed that CCL3 induced mobilization of DC precursors into circulation [37] and detected CCL3 in tumor-infiltrating $CD3^+$ T cells and macrophages after GCV treatment. Therefore, we investigated the roles of CCL3 and its receptors CCR1 and CCR5 in the intratumoral recruitment of DCs and the subsequent establishment of specific tumor immunity. Although CCL4 and CCL5 expression was augmented along with CCL3 expression in tumor sites, the deletion of the *CCL3* gene alone markedly reduced the DC migration, intranodal T cell accumulation, and subsequent Th1 cytokine expression. Similarly, deletion of the *CCL3* gene alone prevented coxsackievirus-induced myocarditis [38], despite enhanced, intracardiac expression of CCL3, CCL4, and CCL5 mRNA [39]. Thus, these three chemokines may form a positive feedback loop, and the deletion of either chemokine might reduce the expression of the others. Moreover, the lack of CCR1 or CCR5 reduces the migration of DCs to tumor sites and subsequent tumor immunity in the draining lymph nodes, such as DC and T cell accumulation and Th1 cytokine expression. As almost all CD11c- and DEC205-positive DCs express CCR1 and CCR5, DC migration may require coordinated and synergistic actions of both of these chemokine receptors.

We have provided definitive evidence regarding the essential contribution of CCL3 and its receptors to apoptosis-induced, specific tumor immunity, which exert their role by attracting DCs to tumor tissues. These observations further suggest that specific tumor immunity can be established more efficiently if some techniques such as chemokine gene transfer can augment the recruitment of immature DCs to apoptotic tumor tissues caused by chemotherapeutic agents and/or irradiation as well as suicide gene therapy.

ACKNOWLEDGMENTS

We thank Dr. Philip M. Murphy (NIAID, NIH) for providing us with CCR1KO mice. We also thank Dr. Toshikazu Kondo (Wakayama Medical University, Wakayama, Japan) for his technical advice about double-color immunofluorescence analysis.

REFERENCES

1. Tsukuma, H., Hiyama, T., Tanaka, S., Nakao, M., Yabuuchi, T., Kitamura, T., Nakanishi, K., Fujimoto, I., Inoue, A., Yamazaki, H., Kawashima, T. (1993) Risk factors for hepatocellular carcinoma among patients with chronic liver disease. *N. Engl. J. Med.* **328**, 1797–1801.
2. Velázquez, R. F., Rodríguez, M., Navascués, C. A., Linares, A., Pérez, R., Sotorríos, N. G., Martínez, I., Rodrigo, L. (2003) Prospective analysis of risk factors for hepatocellular carcinoma in patients with liver cirrhosis. *Hepatology.* **37**, 520–527.
3. Okita, K. (2006) Management of hepatocellular carcinoma in Japan. *J. Gastroenterol.* **41**, 100–106.
4. Poon, R. T., Fan, S. T., Ng, I. O., Lo, C. M., Liu, C. L., Wong, J. (2000) Different risk factors and prognosis for early and late intrahepatic recurrence after resection of hepatocellular carcinoma. *Cancer* **89**, 500–507.
5. Butterfield, L. H. (2004) Immunotherapeutic strategy for hepatocellular carcinoma. *Gastroenterology* **127**, S232–S241.
6. Obeid, M., Tesniere, A., Ghiringhelli, F., Fimia, G. M., Apetoh, L., Perfettini, J. L., Castedo, M., Mignot, G., Panaretakis, T., Casares, N.,

Métivier, D., Larochette, N., van Endert, P., Ciccosanti, F., Piacentini, M., Zitvogel, L., Kroemer, G. (2007) Calreticulin exposure dictates the immunogenicity of cancer cell death. *Nat. Med.* **13,** 54–61.
7. Casares, N., Pequignot, M. O., Tesniere, A., Ghiringhelli, F., Roux, S., Chaput, N., Schmitt, E., Hamai, A., Hervas-Stubbs, S., Obeid, M., Coutant, F., Métivier, D., Pichard, E., Aucouturier, P., Pierron, G., Garrido, C., Zitvogel, L., Kroemer, G. (2005) Caspase-dependent immunogenicity of doxorubicin-induced tumor cell death. *J. Exp. Med.* **202,** 1691–1701.
8. Nowak, A. K., Lake, R. A., Marzo, A. L., Scott, B., Heath, W. R., Collins, E. J., Frelinger, J. A., Robinson, B. W. S. (2003) Induction of tumor cell apoptosis in vivo increases tumor antigen cross-presentation, cross-priming rather than cross-tolerizing host tumor-specific CD8 T cells. *J. Immunol.* **170,** 4905–4913.
9. Hamel, W., Magnelli, L., Chiarugi, V. P., Israel, M. A. (1996) Herpes simplex virus thymidine kinase/ganciclovir-mediated apoptotic death of bystander cells. *Cancer Res.* **56,** 2697–2702.
10. Beltinger, C., Fulda, S., Kammertoens, T., Meyer, E., Uckert, W., Debatin, K. M. (1999) Herpes simplex virus thymidine kinase/ganciclovir-induced apoptosis involves ligand-independent death receptor aggregation and activation of caspases. *Proc. Natl. Acad. Sci. USA* **96,** 8699–8704.
11. Freeman, S. M., Ramesh, R., Marrogi, A. J. (1997) Immune system in suicide-gene therapy. *Lancet* **349,** 2–3.
12. Vile, R. G., Castleden, S., Marshall, J., Camplejohn, R., Upton, C., Chong, H. (1997) Generation of an anti-tumor immune response in a non-immunogenic tumor: HSVtk killing in vivo stimulates a mononuclear cell infiltrate and a Th1-like profile of intratumoural cytokine expression. *Int. J. Cancer* **71,** 267–274.
13. Freeman, S. M., Ramesh, R., Shastri, M., Munshi, A., Jensen, A. K., Marrogi, A. J. (1995) The role of cytokines in mediating the bystander effect using HSV-TK xenogeneic cells. *Cancer Lett.* **92,** 167–174.
14. Chen, S. H., Chen, X. H. L., Wang, Y., Kosai, K., Finegold, M. J., Rich, S. S., Woo, S. L. C. (1995) Combination gene therapy for liver metastasis of colon carcinoma in vivo. *Proc. Natl. Acad. Sci. USA* **92,** 2577–2581.
15. Chen, S. H., Kosai, K., Xu, B., Pham-Nguyen, K., Contant, C., Finegold, M. J., Woo, S. L. C. (1996) Combination suicide and cytokine gene therapy for hepatic metastases of colon carcinoma: sustained antitumor immunity prolongs animal survival. *Cancer Res.* **56,** 3758–3762.
16. Tsuchiyama, T., Nakamoto, Y., Sakai, Y., Marukawa, Y., Kitahara, M., Mukaida, N., Kaneko, S. (2007) Prolonged, NK cell-mediated antitumor effects of suicide gene therapy combined with monocyte chemoattractant protein-1 against hepatocellular carcinoma. *J. Immunol.* **178,** 574–583.
17. Banchereau, J., Steinman, R. M. (1998) Dendritic cells and the control of immunity. *Nature* **392,** 245–252.
18. Sallusto, F., Lanzavecchia, A. (1999) Mobilizing dendritic cells for tolerance, priming, and chronic inflammation. *J. Exp. Med.* **189,** 611–614.
19. Castellino, F., Huang, A. Y., Altan-Bonnet, G., Stoll, S., Scheinecker, C., Germain, R. N. (2006) Chemokines enhance immunity by guiding naïve $CD8^+$ T cells to sites of $CD4^+$ T cell-dendritic cell interaction. *Nature* **440,** 890–895.
20. Dieu, M. C., Vanbervliet, B., Vicari, A., Bridon, J. M., Oldham, E., Aït-Yahia, S., Brière, F., Zlotnik, A., Lebecque, S., Caux, C. (1998) Selective recruitment of immature and mature dendritic cells by distinct chemokines expressed in different anatomic sites. *J. Exp. Med.* **188,** 373–386.
21. Sozzani, S., Luini, W., Borsatti, A., Polentarutti, N., Zhou, D., Piemonti, L., D'Amico, G., Power, C. A., Wells, T. N. C., Gobbi, M., Allavena, P., Mantovani, A. (1997) Receptor expression and responsiveness of human dendritic cells to a defined set of CC and CXC chemokines. *J. Immunol.* **159,** 1993–2000.
22. Sozzani, S. (2005) Dendritic cell trafficking: more than just chemokines. *Cytokine Growth Factor Rev.* **16,** 581–592.
23. Murai, M., Yoneyama, H., Ezaki, T., Suematsu, M., Terashima, Y., Harada, A., Hamada, H., Asakura, H., Ishikawa, H., Matsushima, K. (2003) Peyer's patch is the essential site in initiating murine acute and lethal graft-versus-host reaction. *Nat. Immunol.* **4,** 154–160.
24. Tsuchiyama, T., Kaneko, S., Nakamoto, Y., Sakai, Y., Honda, M., Mukaida, N., Kobayashi, K. (2003) Enhanced antitumor effects of a bicistronic adenovirus vector expressing both herpes simplex virus thymidine kinase and monocyte chemoattractant protein-1 against hepatocellular carcinoma. *Cancer Gene Ther.* **10,** 260–269.
25. Murai, M., Yoneyama, H., Harada, A., Yi, Z., Vestergaard, C., Guo, B., Suzuki, K., Asakura, H., Matsushima, K. (1999) Active participation of $CCR5^+CD8^+$ T lymphocytes in the pathogenesis of liver injury in graft-versus-host disease. *J. Clin. Invest.* **104,** 49–57.
26. Lu, P., Nakamoto, Y., Nemoto-Sakai, Y., Fujii, C., Wang, H., Hashii, M., Ohmoto, Y., Kaneko, S., Kobayashi, K., Mukaida, N. (2003) Potential interaction between CCR1 and its ligand, CCL3, induced by endogeneously produced interleukin-1 in human hepatomas. *Am. J. Pathol.* **162,** 1249–1258.
27. Steinman, R. M., Turley, S., Mellman, I., Inaba, K. (2000) The induction of tolerance by dendritic cells that have captured apoptotic cells. *J. Exp. Med.* **191,** 411–416.
28. Lugade, A. A., Moran, J. P., Gerber, S. A., Rose, R. C., Frelinger, J. G., Lord, E. M. (2005) Local radiation therapy of B16 melanoma tumors increases the generation of tumor antigen-specific effector cells that traffic to the tumor. *J. Immunol.* **174,** 7516–7523.
29. Tang, K. F., Tan, S. Y., Chan, S. H., Chong, S. M., Loh, K. S., Tan, L. K. S., Hu, H. (2001) A distinct expression of CC chemokines by macrophages in nasopharyngeal carcinoma: implication for the intense tumor infiltration by T lymphocytes and macrophages. *Hum. Pathol.* **32,** 42–49.
30. Musha, H., Ohtani, H., Mizoi, T., Kinouchi, M., Nakayama, T., Shiiba, K., Miyagawa, K., Nagura, H., Yoshie, O., Sasaki, I. (2005) Selective infiltration of $CCR5^+CXCR3^+$ T lymphocytes in human colorectal carcinoma. *Int. J. Cancer* **116,** 949–956.
31. Menten, P., Wuyts, A., van Damme, J. (2002) Macrophage inflammatory protein-1. *Cytokine Growth Factor Rev.* **13,** 455–481.
32. Lavergne, E., Combadière, C., Iga, M., Boissonnas, A., Bonduelle, O., Maho, M., Debré, P., Combadiere, B. (2004) Intratumoral CC chemokine ligand 5 overexpression delays tumor growth and increases tumor cell infiltration. *J. Immunol.* **173,** 3755–3762.
33. Fushimi, T., Kojima, A., Moore, M. A., Crystal, R. G. (2000) Macrophage inflammatory protein 3α transgene attracts dendritic cells to established murine tumors and suppresses tumor growth. *J. Clin. Invest.* **105,** 1383–1393.
34. Crittenden, M., Gough, M., Harrington, K., Olivier, K., Thompson, J., Vile, R. G. (2003) Expression of inflammatory chemokines combined with local tumor destruction enhances tumor regression and long-term immunity. *Cancer Res.* **63,** 5505–5512.
35. Yoong, K. F., Afford, S. C., Jones, R., Aujla, P., Qin, S., Price, K., Hubscher, S. G., Adams, D. H. (1999) Expression of CXC and CC chemokines in human malignant liver tumors: a role for human monokine induced by γ-interferon in lymphocyte recruitment to hepatocellular carcinoma. *Hepatology* **30,** 100–111.
36. Walzer, T., Dalod, M., Robbins, S. H., Zitvogel, L., Vivier, E. (2005) Natural-killer cells and dendritic cells: "l'union fait la force". *Blood* **106,** 2252–2258.
37. Zhang, Y., Yoneyama, H., Wang, Y., Ishikawa, S., Hashimoto, S., Gao, J. L., Murphy, P. M., Matsushima, K. (2004) Mobilization of dendritic cell precursors into the circulation by administration of MIP-1α in mice. *J. Natl. Cancer Inst.* **96,** 201–209.
38. Cook, D. N., Beck, M. A., Coffman, T. M., Kirby, S. L., Sheridan, J. F., Pragnell, I. B., Smithies, O. (1995) Requirement for an inflammatory response to viral infection. *Science* **269,** 1583–1585.
39. Gebhard, J. R., Perry, C. M., Harkins, S., Lane, T., Mena, I., Asensio, V. C., Campbell, I. L., Whitton, J. L. (1998) Coxsackievirus B3-induced myocarditis. Perforin exacerbates disease, but plays no detectable role in virus clearance. *Am. J. Pathol.* **153,** 417–428.